

SMALL SYMPLECTIC CAPS AND EMBEDDINGS OF HOMOLOGY BALLS IN THE COMPLEX PROJECTIVE PLANE

JOHN ETNYRE, HYUNKI MIN, LISA PICCIRILLO, AND AGNIVA ROY

ABSTRACT. We present a handlebody construction of small symplectic caps, and hence of small closed symplectic 4-manifolds. We use this to construct handlebody descriptions of symplectic embeddings of rational homology balls in \mathbb{CP}^2 , and thereby provide the first examples of (infinitely many) symplectic handlebody decompositions of a closed symplectic 4-manifold. Our constructions provide a new topological interpretation of almost toric fibrations of \mathbb{CP}^2 in terms of symplectic handlebody decompositions.

1. INTRODUCTION

The literature contains many constructions of closed symplectic 4-manifolds, for example as complex submanifolds of \mathbb{CP}^n , via symplectic reduction, as toric fibrations, or as Lefschetz pencils or fibrations. To be readily compatible however with the tools commonly used by smooth 4-manifold topologists, it is desirable to have a working theory of how to build closed symplectic manifolds out of handles.

We already have a good understanding of handlebody constructions of symplectic fillings by work of Eliashberg [7], Gompf [16] and Weinstein [29]. To get a handle description of a closed symplectic 4-manifold, one might want to glue a such a filling to symplectic cap along a fixed contact 3-manifold. But there is presently no fully handle-theoretic construction for symplectic caps; because Weinstein 4-manifolds only have handles of index at most 2, there are no Weinstein 3- and 4-handles. Moreover, existing constructions of symplectic caps, e.g. [9], nearly always produce caps with large homology. Developing a practical handle theoretic construction of small symplectic caps is the primary goal of this paper.

Our construction of small symplectic caps relies on a technique of Gay [13] from 2002. Gay's technique suggests building symplectic caps by attaching particular 2-handles (called a *convex-concave handle*, see Section 2.5) to the convex boundary of a symplectic filling. As the name suggests, after attaching a convex-concave 2-handle one has a symplectic 4-manifold with concave boundary. That concave boundary can then be capped with an (upside down) Weinstein handlebody to obtain a closed symplectic manifold.

Building closed symplectic manifolds in this way was the original intended purpose of Gay's technique, but to date it has not been carried out because it is difficult to identify the concave boundary produced after the convex-concave 2-handle attachment. Even when one can identify the resulting contact 3-manifold, it is frequently overtwisted, and hence does not even admit a weak symplectic filling. In this paper, we use recent developments

in contact 3-manifold topology, notably [10], to get past these technical issues in certain circumstances.

As a demonstration of how one might work with our symplectic caps in practice, we use them to construct hypersurfaces of contact type in \mathbb{CP}^2 (equivalently, construct symplectic embeddings in \mathbb{CP}^2 that the hypersurfaces bound). Understanding the settings in which 3-manifolds embed in 4-manifolds is a hard problem with rich history in both the smooth and symplectic categories. Perhaps the easiest setting to study is for the simplest 3-manifolds, lens spaces, and the simplest closed 4-manifold in which they can embed, \mathbb{CP}^2 . In the smooth category little is known. For example, it is unknown whether four distinct lens spaces can be (disjointly) embedded in \mathbb{CP}^2 . In contrast, in the symplectic category this problem is completely understood. In fact, Vianna [26] used almost toric fibrations and constructed a family of three disjoint lens spaces that are embedded in \mathbb{CP}^2 as hypersurfaces of contact type (equivalently, three rational homology balls that symplectically embed in \mathbb{CP}^2). Evans and Smith [12] then proved that Vianna's are the only hypersurfaces of contact type among all families of lens spaces in \mathbb{CP}^2 . Recently, Lisca and Parma [21] gave a smooth interpretation of Vianna's embeddings using "horizontal" handle decompositions (Section 4.1). We give a new symplectic interpretation of Vianna's embeddings using symplectic handle decompositions.

Theorem 1.1. *For any Markov triple (p_1, p_2, p_3) there exists a triple of integers (q_1, q_2, q_3) such that the three rational homology 4-balls B_{p_i, q_i} are disjointly symplectically embedded in \mathbb{CP}^2 . Furthermore, the Weinstein handle decompositions of the rational homology balls are sub-decompositions of an explicit symplectic handle decomposition of \mathbb{CP}^2 .*

See Section 2.1 for the definition of Markov triples, Figure 1 for the rational homology ball $B_{p,q}$ and Definition 2.10 for the formal definition of a symplectic handle decomposition.

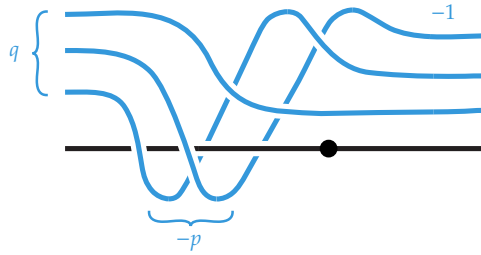


FIGURE 1. The rational ball $B_{p,q}$ has boundary the lens space $L(p^2, pq-1)$. The -1 framing on the 2-handle is relative to the torus framing. Here and throughout, figures should be braided closed.

Our techniques can be used to construct many other embeddings of contact lens spaces as hypersurfaces of contact type in $\mathbb{CP}^2 \# n\overline{\mathbb{CP}^2}$, which we do not record here. Ultimately,

we hope that with further study our techniques can be used to construct other, possibly exotic, small symplectic manifolds.

We outline the proof of Theorem 1.1 now. The main technical work lies in defining a convex-concave 2-handle between standard contact structures on (connected sums of) lens spaces. To do this, we attach a convex-concave 2-handle to the symplectization of a standard contact lens space to obtain a symplectic cobordism with two concave boundary components. One boundary component is the original lens space, the other is a connected sum of two lens spaces. In Section 3.2, we show that the contact structure induced on the reducible boundary component is equivalent to the result of Legendrian surgery on some Legendrian torus knot in an overtwisted lens space; this allows us to conclude that the contact manifold is a connected sum of standard contact lens spaces. This cobordism can then be capped off by Weinstein fillings B_{p_i, q_i} of standard contact lens spaces to obtain a closed symplectic manifold. We denote the resulting symplectic manifold by $(X_{p_1, p_2, p_3}, \omega_{p_1, p_2, p_3})$. In Section 4 we use horizontal handlebody decompositions, introduced by Lisca and Parma [20], to show that X_{p_1, p_2, p_3} is diffeomorphic to \mathbb{CP}^2 . A theorem of Taubes [25] then guarantees that $(X_{p_1, p_2, p_3}, \omega_{p_1, p_2, p_3})$ is deformation equivalent to \mathbb{CP}^2 .

In Section 5 we give two additional proofs that X_{p_1, p_2, p_3} is diffeomorphic to \mathbb{CP}^2 . The first of these, inspired by Vianna [26], inductively identifies our spaces X_{p_1, p_2, p_3} with \mathbb{CP}^2 . The second uses a handlebody description of almost toric fibrations to exhibit the diffeomorphism. We conclude the paper by showing that this almost toric fibration structure on X_{p_1, p_2, p_3} indeed agrees with the almost toric structures that Vianna used to build the original embeddings of the rational homology balls.

Theorem 1.2. *An almost toric fibration of \mathbb{CP}^2 for given Markov triple (p_1, p_2, p_3) is compatible with the symplectic handlebody decomposition from Theorem 1.1, i.e. the restriction on each of sub-handlebodies, B_{p_i, q_i} and the pants cobordism is also an almost toric fibration.*

Organization. In Section 2, we collect the background material we will need. In Section 3, we build symplectic pants cobordisms between a standard contact lens space and a disjoint union of two standard contact lens spaces and construct the symplectic manifolds X_{p_1, p_2, p_3} into which the rational homology balls B_{p_i, q_i} embed. In Section 4, we draw a handle diagram for X_{p_1, p_2, p_3} and prove that the result is \mathbb{CP}^2 equipped with the standard symplectic structure. This proves Theorem 1.1. In Section 5, we exhibit two other proofs that X_{p_1, p_2, p_3} is \mathbb{CP}^2 and prove Theorem 1.2.

Conventions. The lens space $L(p, q)$ is defined to be the $-p/q$ Dehn surgery on the unknot. We define $B_{p, q}$ to be a smoothing of the cyclic quotient singularity of type $(p^2, pq - 1)$. For a handle diagram description of this manifold, see Figure 4.

Acknowledgements. JE and AR were partially supported by DMS-1906414 and DMS-2203312. JE was also partially supported by the Georgia Institute of Technology's Elaine M. Hubbard Distinguished Faculty Award. LP was partially supported in part by a Sloan Fellowship, a Clay Fellowship, and the Simons collaboration "New structures in low-dimensional topology". Part of this work was done during Graduate Student Topology

and Geometry Conference in 2022. JE, HM and AR are grateful to Georgia Tech for the support during this conference. The authors thank Paolo Lisca and Andrea Parma for helpful correspondence about Theorem 4.2, and Nicki McGill, Bülent Tosun, and Morgan Weiler for useful conversations about several aspects of this paper.

2. PRELIMINARIES

In this section we review the background results necessary for our main results. In Section 2.1, we recall the definition of a Markov triple and discuss how to generate all such triples. Transverse surgery is reviewed in Section 2.2 and we discuss torus knots in lens spaces in Section 2.4. In Section 2.3, we recall the definition of and basic facts about rational open book decompositions. Various types of symplectic handle attachments are discussed in Section 2.5 while Weinstein rational homology balls are built in Section 2.6. Finally we discuss contact structures on lens spaces in Section 2.7.

2.1. Markov triples and the Markov tree. A *Markov triple* is a triple of positive integers (p_1, p_2, p_3) satisfying

$$p_1^2 + p_2^2 + p_3^2 = 3p_1p_2p_3.$$

We note that if (p_1, p_2, p_3) is a Markov triple, then so are the triples $(p_2, p_3, 3p_2p_3 - p_1)$ and $(p_1, p_3, 3p_1p_3 - p_2)$ and these are called *mutations* of the original triple. We can use these relation to build the *Markov tree*. This is a binary tree with Markov triples (p_1, p_2, p_3) as vertices for $p_1 \leq p_2 \leq p_3$ and an edge connecting two vertices related by mutation. Specifically the root of the tree is $(1, 1, 1)$ which has a single child vertex $(1, 1, 2)$. The vertex $(1, 1, 2)$ also has a single child vertex $(1, 2, 5)$. Any other vertex (p_1, p_2, p_3) has two child vertices; the left child is $(p_2, p_3, 3p_2p_3 - p_1)$, and the right child is $(p_1, p_3, 3p_1p_3 - p_2)$, see Figure 2.

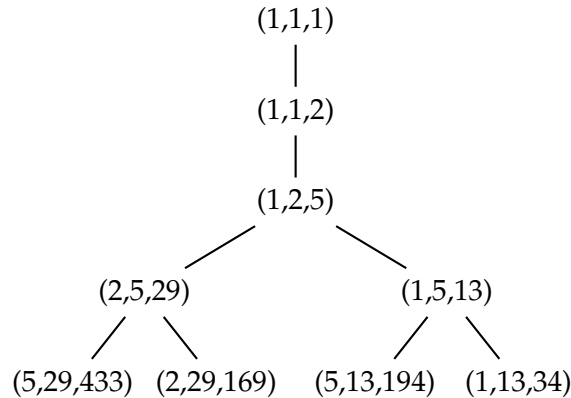


FIGURE 2. The Markov tree.

2.2. Transverse surgery. Let K be a transverse knot in a contact 3-manifold (M, ξ) . There exist polar coordinates (r, θ, ϕ) on a neighborhood of K such that the contact form α of ξ can be written as

$$\alpha = r^2 d\theta + d\phi$$

where K is identified with the ϕ -axis and $r \in [0, R)$ for some $R > 0$. For any negative rational number a with $\sqrt{-1/a} < R$, we call $S_a = \{r \leq \sqrt{-1/a}\}$ a *standard neighborhood of K with slope $-1/a$* . Notice that the characteristic foliation on ∂S_a is the linear foliation with slope a .

A *transverse surgery* on (K, S_a) is a surgery operation to produce a new contact manifold. There are two types of transverse surgeries: *admissible* and *inadmissible* transverse surgeries. For more details, see [4, 6]. In general, the resulting contact structure of transverse surgery depends on the choice of a neighborhood S_a . In particular, we can only perform admissible transverse s -surgery for $s < a$ (notice that the polar coordinates on S_a determines the framing of K). If there is an obvious choice of a neighborhood for K , then we omit S_a and just talk about admissible transverse surgery on K .

Conway [6] showed that inadmissible transverse surgery is equivalent to some contact surgery on its Legendrian approximations. In some cases, this is also true for admissible transverse surgery. This is explored in [4, Lemma 3.16], and a simple case of that theorem yields the following result.

Proposition 2.1. *Let S_a be a standard neighborhood of the transverse knot K . If $s = \lfloor a \rfloor - 1$, then admissible transverse s -surgery on K is equivalent to Legendrian surgery on a Legendrian approximation of K in S_a .*

2.3. Rational open book decompositions. Here, we briefly review rational open book decompositions and their compatible contact structures. For more details, see [3].

Definition 2.2. A *rational open book decomposition* for a 3-manifold M is a pair (\mathcal{B}, π) consisting of an oriented link $\mathcal{B} = (K_1, \dots, K_n)$ in M and a fibration $\pi : (M \setminus \mathcal{B}) \rightarrow S^1$ such that for any $\theta \in S^1$ and a neighborhood N_i of K_i , $\pi^{-1}(\theta) \cap \partial N_i$ is not a meridian. We say \mathcal{B} is the *binding* of the open book decomposition and each $\overline{\pi^{-1}(\theta)}$ is page of the open book decomposition. If $\overline{\pi^{-1}(\theta)}$ is a Seifert surface for \mathcal{B} then we call (\mathcal{B}, π) an open book decomposition, or sometimes an *honest* open book decomposition.

Notice in the definition above, there is some surface Σ and a map $f : \Sigma \rightarrow M$ such that f , on the interior of Σ , parameterizes $\pi^{-1}(\theta)$ and $\partial \Sigma$ maps to \mathcal{B} , the restriction of f to each component of $\partial \Sigma$ is a cover of a component of \mathcal{B} . We orient the pages of the open book decomposition (and Σ by f) so that f restricted to each component of $\partial \Sigma$ has positive degree, or in other words a positively oriented vector to $\partial \Sigma$ maps to a positively oriented vector on \mathcal{B} .

Definition 2.3. A (rational) open book decomposition (\mathcal{B}, π) *supports* a contact 3-manifold $(M, \xi_{\mathcal{B}})$ if there exists a contact form α satisfying

- $\ker \alpha$ is isotopic to $\xi_{\mathcal{B}}$,
- $\alpha(v) > 0$ for any positively oriented tangent vector $v \in T\mathcal{B}$ and
- $d\alpha$ is a positive volume form of each page.

Let K be a binding component of a (rational) open book decomposition (\mathcal{B}, π) of M and let N be a neighborhood of K . Fix a reference framing on K . Then $\pi|_{M \setminus N}^{-1}(\theta) \cap \partial N$ is an essential simple closed curve on ∂N . We say the slope of this curve with respect to the reference framing is the *page slope* of K . The following theorem shows that for sufficiently small slopes, the resulting contact structure of admissible transverse surgery on K is supported by essentially the same open book.

Proposition 2.4 (Baker–Etnyre–Van-Horn-Morris [3]). *Suppose K is a binding component of a (rational) open book decomposition (\mathcal{B}, π) supporting $(M, \xi_{\mathcal{B}})$. Then for any $r \in \mathbb{Q}$ less than the page slope of K , the resulting contact structure of admissible transverse r -surgery on K is supported by (\mathcal{B}^*, π) where \mathcal{B}^* is the surgery dual of \mathcal{B} .*

The following lemma was proven in [4, 11] for honest open book decompositions but the same proof works for rational open book decompositions.

Lemma 2.5. *Let (\mathcal{B}, π) be a (rational) open book decomposition supporting $(M, \xi_{\mathcal{B}})$.*

- (1) *A standard neighborhood S_a of each binding component can be chosen so that a becomes arbitrarily close to the page slope (which is measured by the framing induced from the polar coordinates of S_a).*
- (2) *The complement of the binding is universally tight. Moreover, it does not contain Giroux torsion, but will remain tight when Giroux torsion is added.*

We finish this section by introducing a lemma which will be used in later sections.

Lemma 2.6. *Let (\mathcal{B}, π) be a (rational) open book decomposition supporting $(M, \xi_{\mathcal{B}})$. Then there is a contact form α for $\xi_{\mathcal{B}}$ and polar coordinates (r, θ, ϕ) near each binding component such that*

$$\alpha = \frac{1}{Ar^2 + B}(r^2 d\theta + d\phi)$$

and the projection map is

$$\pi(r, \theta, \phi) = C\theta + D\phi$$

for some constants A, B, C, D .

Proof. Since a binding component is a transverse knot, we can choose polar coordinates (r, θ, ϕ) near a binding component such that

$$\alpha = \frac{1}{Ar^2 + B}(r^2 d\theta + d\phi).$$

for some constants A and B . After perturbation, we can further assume that π is linear near each binding component with respect to the coordinates (r, θ, ϕ) , so we can write

$$\pi = C\theta + D\phi$$

for some constants C and D . □

2.4. Torus knots in lens spaces. For any relatively prime integers r and s , we define a lens space $L(r, s)$ by

$$L(r, s) = S_U^3(-r/s)$$

where U is the unknot in S^3 and $S_U^3(-r/s)$ denotes $-r/s$ Dehn surgery on U . Let T be a Heegaard torus of S^3 which is the boundary of a neighborhood of U . Let (λ_U, μ_U) be the coordinates on T where μ_U is a meridian and λ_U is the Seifert longitude of U . By observing that T is still a Heegaard torus of the lens space $L(r, s)$ obtained by surgery on U , we can keep using (λ_U, μ_U) as coordinates for the Heegaard torus in $L(r, s)$.

We now set up some convenient terminology. For any relatively prime integers p and q , we define a (p, q) -torus knot $T_{p,q}$ in $L(r, s)$ to be a simple closed curve on T in the homology class $p\lambda_U + q\mu_U$. We say $T_{p,q}$ is a *positive* torus knot if $0 < q/p < -r/s$ when $-r/s > 0$, or $q/p < -r/s < 0$ or $-r/s < 0 < q/p$ and $-r/s < 0$ (which is equivalent to q/p being counterclockwise of $-r/s$ and clockwise of 0 in the Farey graph, see Section 2.7), and a *negative* torus knot if $-r/s < q/p < 0$ when $-r/s < 0$, or $0 < -r/s < q/p$ or $q/p < 0 < -r/s$ when $-r/s > 0$ (which is equivalent to q/p being clockwise of $-r/s$ and counterclockwise of 0 in the Farey graph, see Section 2.7). We also say $T_{p,q}$ is *trivial* if $|pr + qs| = 1$ or $|q| = 1$, and otherwise, *nontrivial*. Notice that a trivial torus knot is isotopic to one of the cores of the Heegaard tori. The framing for $T_{p,q}$ induced from the Heegaard torus T is called the *torus framing* of $T_{p,q}$ and is denoted by f_T .

Baker, Van-Horn-Morris, and the first author showed that every torus knot in any lens space is rationally fibered.

Lemma 2.7 (Baker–Etnyre–Van-Horn-Morris [3]). *A torus knot $T_{p,q}$ in a lens space $L(r, s)$ is a rationally fibered knot. Moreover,*

- *the torus framing is larger than the page slope for positive torus knots,*
- *the torus framing is less than the page slope for negative torus knots,*

and if the torus knot is nontrivial, then the page and torus framings differ by more than one.

One may see why this is true (especially the last statement) by noting that $L(r, s)$ is the union of two solid tori S_1 and S_2 and that a (rational) Seifert surface for $T_{p,q}$ can be built by taking some number of meridional disks in S_1 and some other number in S_2 and then resolving their intersections on $\partial S_1 = \partial S_2$ in either a positive or negative way. In the case $T_{p,q}$ is null-homologous, each resolution contributes ± 1 to the difference between the torus and Seifert framing. This is similar when $T_{p,q}$ is only rationally null-homologous, except that the “Seifert framing” is not exactly a framing.

2.5. Symplectic handle attachments. Here we review symplectic 2-handles constructed by Gay [13]. First, for an n -dimensional k -handle $H = D^k \times D^{n-k}$, we denote the attaching region $\partial D^k \times D^{n-k}$ by $\partial_- H$ and denote $D^k \times \partial D^{n-k}$ by $\partial_+ H$. Also, we orient $\partial_- H$ as the opposite of the boundary orientation and orient $\partial_+ H$ as the usual boundary orientation. These are the orientations one would choose if they wanted to think of the k -handle as a (rel. boundary) cobordism from ∂_- to ∂_+ .

Definition 2.8. Let H be a 4-dimensional k -handle and ω_H be a symplectic structure on H .

- (H, ω_H) is a *symplectic k -handle with convex boundaries* if there is a Liouville vector field on H that points into H along $\partial_- H$ and out of H along $\partial_+ H$. We also call it a *convex k -handle* in short.
- (H, ω_H) is a *symplectic k -handle with concave boundaries* if there is a Liouville vector field on H that points out of H along $\partial_- H$ and into H along $\partial_+ H$. We also call it a *concave k -handle* in short.

We note that convex handles can be attached to a convex boundary to create a new symplectic manifold that also has a convex boundary, and similarly for concave handles.

Example 2.9. Weinstein k -handles are convex k -handles for $k = 0, 1, 2$. By turning them upside down, we obtain concave $(4 - k)$ -handles.

Notice that we cannot build a closed symplectic manifold using just concave or convex handles. In [13], Gay showed how to attach a 2-handle to a convex boundary to create a symplectic manifold with concave boundary. We will describe his work below, but we will call his handle attachment a *convex-concave 2-handle*. We note now that one can hope to build a closed symplectic manifold by using convex handles, then one convex-concave 2-handle and then several concave handles. A main goal of this paper is to show that this strategy can indeed be carried out.

Definition 2.10. We say a symplectic 4-manifold (X, ω) admits a *symplectic handlebody decomposition* if it admits a handlebody decomposition consisting of convex, concave, and convex-concave handles.

The construction of Gay's convex-concave 2-handles is somewhat similar to the Weinstein handle construction [29], but a convex-concave handle requires a pair of dilating and contracting Liouville vector fields. The model handle is defined as a subset of (\mathbb{R}^4, ω_0) , where $\omega_0 = r_1 dr_1 d\theta_1 + r_2 dr_2 d\theta_2$ is the standard symplectic structure with polar coordinates $(r_1, \theta_1, r_2, \theta_2)$. Consider the function $f(r_1, \theta_1, r_2, \theta_2) = -r_1^2 + r_2^2$. For positive integers C and D , the Liouville vector fields X_- and X_+ are defined by

$$X_- = \left(\frac{r_1}{2} - \frac{C}{r_1} \right) \frac{\partial}{\partial r_1} + \frac{r_2}{2} \frac{\partial}{\partial r_2},$$

$$X_+ = -\frac{r_1}{2} \frac{\partial}{\partial r_1} - \left(\frac{1}{2} r_2 - \frac{D}{r_2} \right) \frac{\partial}{\partial r_2}.$$

X_- is a dilating Liouville vector field transverse to $f^{-1}(y)$ for $-2D < y < 0$ and X_+ is a contracting Liouville vector field transverse to $f^{-1}(y)$ for $0 < y < 2C$. Now we define the handle H as a subset of $f^{-1}[-2D, 2C]$ such that $\partial_- H$ is a subset of $f^{-1}(-2D + \epsilon)$ and $\partial_+ H$ consists of a subset of $f^{-1}(2C - \epsilon)$ and a certain interpolation from $f^{-1}(-2D + \epsilon)$ to $f^{-1}(2C - \epsilon)$. See Figure 3.

Unlike Weinstein 2-handles, the attaching sphere $\partial_- H \cap \{r_2 = 0\}$ is a transverse knot. Also, they can only be attached along a special transverse link to make the entire result concave.

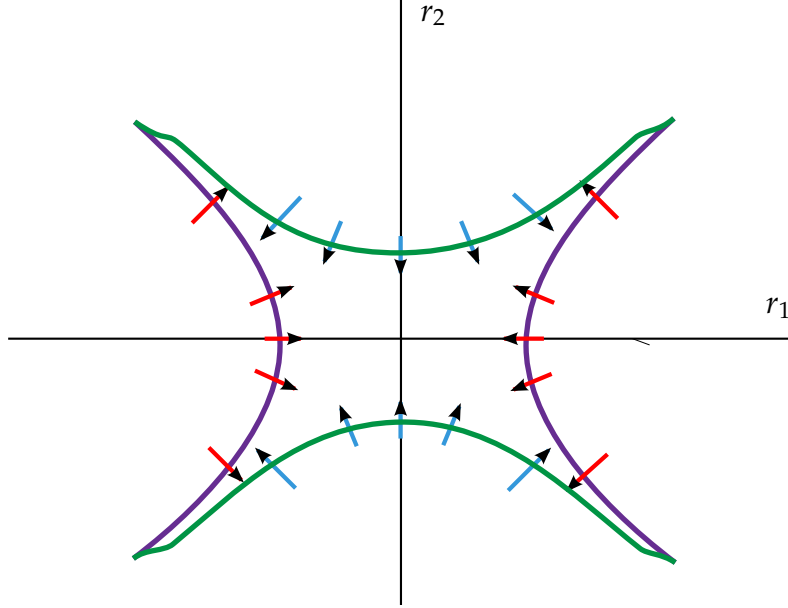


FIGURE 3. A model for a convex-concave handle in (\mathbb{R}^4, ω_0)

Definition 2.11. A transverse link $\mathcal{K} \subset (M, \xi)$ is *nicey fibered* if there exists a fibration $p: M \setminus \mathcal{K} \rightarrow S^1$ and a contact vector field X on M such that

- X is transverse to the fibers of p
- For each binding component K , there are polar coordinates (r, θ, ϕ) on a neighborhood of K such that
 - $\partial/\partial r$ is tangent to the fibers.
 - $dr(X) = 0$.
 - X and dp are both invariant under $\partial/\partial r, \partial/\partial \theta$ and $\partial/\partial \phi$.
- Let X be a coorientation of both ξ and the fibers. Then the characteristic foliation on the fiber near each binding component K points in towards K .

Now let $\mathcal{K} = (K_1, K_2, \dots, K_m)$ be a nicely fibered link in (M, ξ) (equipped with a reference framing) and let $\mathbf{n} = (n_1, n_2, \dots, n_m)$ be integers that are greater than the fiber slopes of each link component.

Theorem 2.12 (Gay [13]). *With the notation above, let (W, ω) be a strong symplectic filling of (M, ξ) . Then there exist a strong symplectic cap (W', ω') containing (W, ω) , obtained by attaching n_i -framed convex-concave 2-handles (H_i, ω_i) along all K_i .*

2.6. Lens spaces bounding rational homology balls. Recall that $B_{p,q}$ is a smoothing of the cyclic quotient singularity of type $(p^2, pq - 1)$, i.e. $B_{p,q}$ is a smoothing of the quotient of $B^4 \subset \mathbb{C}^2$ under the \mathbb{Z}_{p^2} -action generated by

$$(z_1, z_2) \mapsto (e^{2\pi i/p^2} z_1, e^{2\pi(pq-1)i/p^2} z_2).$$

It is a rational homology ball and can be described by a handlebody diagram, as shown in Figure 4. For more details, see [19, 28].

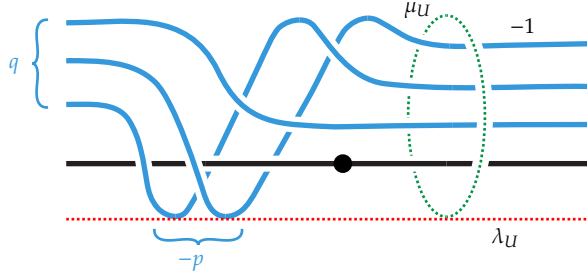


FIGURE 4. The rational ball $B_{p,q}$ has boundary the lens space $L(p^2, pq - 1)$. The red longitude is oriented left right and the green meridian is oriented clockwise. The -1 framing on the 2-handle is relative to the torus framing (note the blue curve sits on a Heegaard torus).

Lemma 2.13. *The boundary of $B_{p,q}$ is the lens space $L(p^2, pq - 1)$.*

There are several standard arguments for proving this; we will present a proof which uses a method we will rely on heavily later in the paper. We will require the following classical lemma, see for instance [23, Lemma 9.I.4].

Lemma 2.14. *Let M be a 3-manifold with a Heegaard splitting $V_1 \sqcup_{\phi} V_2$ where V_i are genus g handlebodies that are glued together by a diffeomorphism $\phi : \partial V_1 \rightarrow -\partial V_2$. Let γ be a simple closed curve on ∂V_1 , and suppose M' is obtained by Dehn surgering M along γ with framing $f_{\partial V_1} \pm 1$. Then M' has a Heegaard splitting $V_1 \sqcup_{\tau_{\gamma}^{\pm 1} \circ \phi} V_2$, where τ_{γ} denotes the right-handed Dehn twist of ∂V_1 along γ .*

Proof of Lemma 2.13. Let μ_U and λ_U be the two oriented curves in the boundary $\partial(B_{p,q})$ shown in Figure 4. If we ignore the blue curve in the figure then the boundary manifold is $S^1 \times S^2$ and is the union of two solid tori. The first, V_1 , is a neighborhood of the black curve and the second, V_2 , is its complement. Notice that λ_U bounds a disk in the outside solid torus. We can think of $\partial(B_{p,q})$ as the result of surgery along the blue knot in $S^1 \times S^2$. Since the blue knot lies on a Heegaard torus for $S^1 \times S^2$ and we surger the blue knot with 1 less than the Heegaard torus framing, performing the blue surgery has the effect of modifying the gluing map of the Heegaard splitting as indicated in Lemma 2.14. So we see that $\partial(B_{p,q})$ is a lens space.

To compute which lens space, we will determine which simple closed curve in ∂V_2 bounds a disk in the inside solid torus. Observe that the 0-framed push-off of the black knot bounds a disk in V_1 , this is the curve λ_U thought of as sitting on a torus just inside the blue curve. We will now isotope λ_U “past” the blue surgered curve, and identify it in ∂V_2 . Pushing past the blue curve yields $\lambda_U - p(-p\mu_U + q\lambda_U) = p^2\mu_U + (1 - pq)\lambda_U$. Thus we conclude that $\partial(B_{p,q})$ is the lens space $L(p^2, pq - 1)$. \square

Remark 2.15. We collect a few facts we will require about $B_{p,q}$.

- (1) The rational homology ball $B_{p,q}$ admits Weinstein structures for each $\pm\xi_{std}$. See Figure 5 for Weinstein handlebody diagrams.

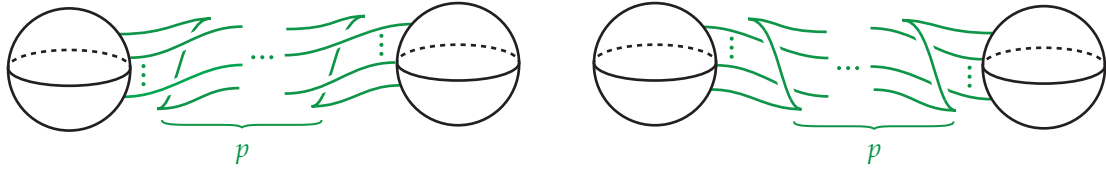


FIGURE 5. Weinstein $B_{p,q}$ for $(L(p^2, pq - 1), \xi_{std})$ and $(L(p^2, pq - 1), -\xi_{std})$, there are q strands.

- (2) The contactomorphism $\tau: L(p^2, pq - 1) \rightarrow L(p^2, pq - 1)$ from Corollary 2.19 below extends to a diffeomorphism of $\bar{\tau}: B_{p,q} \rightarrow B_{p,q}$. This follows immediately from the definition of τ .
- (3) Because we will make use of such computations later, we also compute for reference the image of the meridian μ_U of black curve in Figure 4 when we push it past the blue surgery; here we see $\mu_U \mapsto (1 + pq)\mu_U - q^2\lambda_U$. So if we take (λ_U, μ_U) to be a basis for $H_1(T^2)$, then the matrix describing the images of the longitude and meridian of the black curve after isotoping past the blue surgery curve is

$$\begin{pmatrix} 1 - pq & -q^2 \\ p^2 & 1 + pq \end{pmatrix}.$$

2.7. Contact structures on lens spaces and decorated paths. Here, we review how to build a contact structure on a lens space. To do so, we first review the Farey graph. First, we define the *Farey sum* of two rational numbers to be

$$\frac{a}{b} \oplus \frac{c}{d} := \frac{a + c}{b + d}.$$

Also, we define *Farey multiplication* of two rational numbers to be

$$\frac{a}{b} \bullet \frac{c}{d} := ad - bc.$$

Now consider the Poincaré disk in \mathbb{R}^2 equipped with the hyperbolic metric. Label the points $(0, 1)$ by $0 = 0/1$ and $(0, -1)$ by $\infty = 1/0$ and add a hyperbolic geodesic between the two points. Take the half circle with non-negative x coordinate. Label any point half-way between two labeled points with the Farey sum of the two points and connect it to

both points by a geodesic. Iterate this process until all the positive rational numbers are a label on some point on the half circle. Now do the same for the half circle with non-positive x coordinate (for ∞ , use the fraction $-1/0$). See Figure 6. We note that for two points on the Farey graph labeled r and s , respectively, we have $|r \bullet s| = 1$ if and only if there is an edge between them.

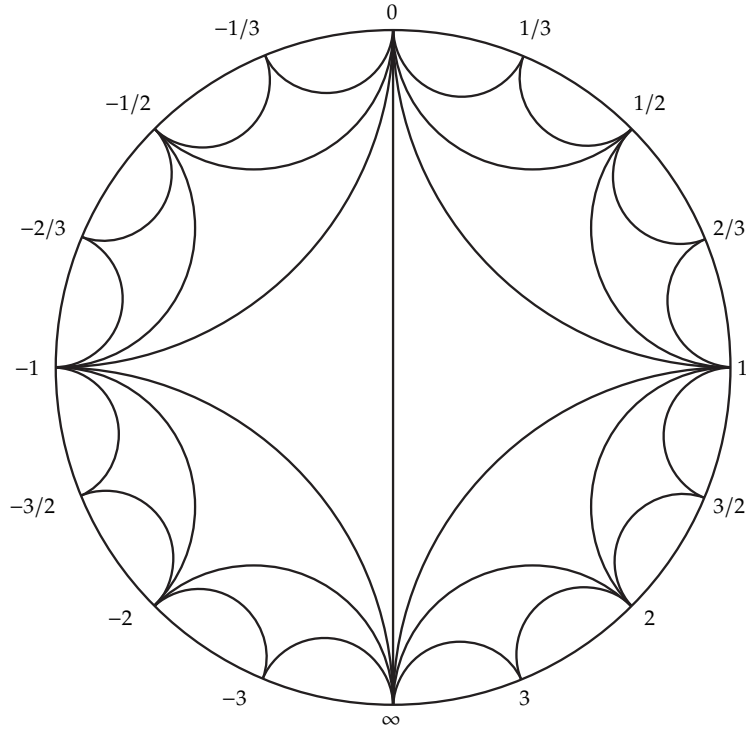


FIGURE 6. The Farey graph.

Given a rational number q/p we denote by $(q/p)^c$ is the largest rational number q'/p' satisfying $pq' - p'q = -1$ and by $(q/p)^a$ is the smallest rational number q''/p'' satisfying $pq'' - p''q = 1$. Notice that this means there is an edge from q/p to $(q/p)^c$ and to $(q/p)^a$. One may also show that there is an edge between $(q/p)^c$ and $(q/p)^a$.

A *path* from r to s in the Farey graph is a series of rational numbers $\{r = s_0, s_1, \dots, s_n = s\}$ moving clockwise from r to s so that s_i and s_{i+1} are connected by an edge in the Farey graph. We say a path $P = \{s_0, s_1, \dots, s_n\}$ is *minimal* if $|s_i \bullet s_j| = 1$ if and only if $j = i \pm 1$. Suppose P is not minimal, that is, $|s_i \bullet s_{i+k}| = 1$ for some $k > 1$. Then we can *shorten* the path by removing $s_{i+1}, \dots, s_{i+k-1}$ and obtain a new path $P' = \{s_1, \dots, s_i, s_{i+k}, \dots, s_n\}$. A *decorated path* is a path in the Farey graph such that each edge between two consecutive points is assigned the $+$, $-$, or \circ sign.

We will use decorated paths in the Farey graph to describe contact structures on some 3-manifolds. We assume the reader is familiar with convex surface theory as can be found in [17], but we recall that a convex surface has dividing curves (which are a collection of

embedded curves that separate the surface into two parts) that essentially determine the contact structure in a neighborhood of the surface. A *basic slice* $B_{\pm}(s, s')$ is defined to be a minimally twisting contact structure on $T^2 \times I$ with convex boundary with two dividing curves of slopes s and s' , where s' is clockwise of s and $|s \bullet s'| = 1$. There are two non-isotopic contact structures satisfying such conditions and they differ by their coorientation. We denote one by $B_+(s, s')$ and the other by $B_-(s, s')$ and call them a positive and negative basic slice, respectively. Since $|s \bullet s'| = 1$, there is an edge between s and s' . Thus we can describe a basic slice $B_{\pm}(s, s')$ as a decorated path ($s_0 = s, s_1 = s'$), consisting of a single edge between s and s' , and the sign of the edge is the sign of the basic slice.

It will be useful to have flexibility in the coordinate used on the boundary of a solid torus. To allow for this we describe a solid torus as follows. Consider $T^2 \times [0, 1]$ and choose some basis for the homology of T^2 . The *solid torus with lower meridian of slope r* is formed from $T^2 \times [0, 1]$ by collapsing the leaves of a foliation of $T^2 \times \{0\}$ by circles of slope r . We denote this solid torus S_r . We can similarly define the *solid torus with upper meridian of slope r* similarly except we collapse leaves of the same foliation on $T^2 \times \{1\}$ and denote the result S^r .

We will now consider tight contact structures on a solid torus S_r with boundary being convex with two dividing curves of slope s . We will denote such a contact structure by $S_r(s)$. Similarly $S^r(s)$ will denote a tight contact structure on a solid torus S^r with convex boundary having two dividing curves of slope s .

Kanda [18] showed that there exists a unique tight contact structure on $S_r(s)$ and $S^r(s)$ up to isotopy fixing boundary if $|s \bullet r| = 1$. Since there is an edge between r and s in the Farey graph, we can describe the tight contact structure on $S_r(s)$ as a decorated path ($s_0 = r, s_1 = s$), consisting of a single edge between r and s , and the sign of the edge is \circ . For $S^r(s)$, we use ($s_0 = s, s_1 = r$) instead.

Next, we described any tight contact structure on $S_r(s)$ and $S^r(s)$ for any $r, s \in \mathbb{Q}$. Let $(r = s_0, \dots, s_n = s)$ be the minimal path from r to s in the Farey graph. Then we can decompose a tight contact structure on $S_r(s)$ into

$$S_r(s) = S_r(s_1) \cup B(s_1, s_2) \cup \dots \cup B(s_{n-1}, s_n).$$

Thus we can describe a tight contact structure on $S_l(r, s)$ using a decorated path by assigning \circ to the edge (s_0, s_1) and assigning $+$ or $-$ to all other edges (s_i, s_{i+1}) according to the sign of the basic slice $B(s_i, s_{i+1})$ for $1 \leq i \leq n-1$. For $S^r(s)$, we use the path $(s = s_0, \dots, s_n = r)$ instead and it is the last edge in the path that is assigned a \circ while the others have a $+$ or a $-$. Giroux [15] and Honda [17] proved that any tight contact structure on $S_r(s)$ or $S^r(s)$ can be described this way.

By gluing $S_{-r/s}(p/q)$ and $S^0(p/q)$ together along the boundary, we can construct a contact structure on $L(r, s)$ and describe it using a decorated path $P = \{s_0 = -r/s, \dots, s_n = p/q, \dots, s_m = 0\}$ in the Farey graph where the first and last edges of the path are decorated with \circ and the rest by a $+$ or $-$.

Giroux [15] and Honda [17] classified tight contact structures on lens spaces. We can state part of their classification in terms of decorated paths in the Farey graph.

Theorem 2.16 (Giroux [15], Honda [17]). *Let ξ be a contact structure on $L(r, s)$ and P is the corresponding decorated path from $-r/s$ to 0 in the Farey graph. Then*

- (1) *if P is minimal, then ξ is tight.*
- (2) *if P is minimal and all edges have the same sign except for the first and the last ones which are decorated with \circ , then ξ is universally tight.*
- (3) *if P is minimal and contains both $+$ and $-$ signs, then ξ is tight but virtually overtwisted.*
- (4) *if P is not minimal and there are two adjacent edges (s_{i-1}, s_i) and (s_i, s_{i+1}) with different signs that can be shortened (i.e. $|s_{i-1} \cdot s_{i+1}| = 1$), then ξ is overtwisted.*

See Figure 7 for an example of an overtwisted contact structure on $L(3, 1)$ obtained by gluing $S_{-3}(-8/5)$ and $S^0(-8/5)$ together.

According to the previous theorem, there exist two universally tight contact structures on $L(p, q)$ and they differ by coorientation. We denote them by ξ_{std} and $-\xi_{std}$, and call them the *standard contact structures* on $L(p, q)$.

Remark 2.17. In this paper, we will not strictly distinguish ξ_{std} and $-\xi_{std}$, since they are contactomorphic (see Corollary 2.19). When we refer to a standard contact structure on $L(p, q)$, it could be either ξ_{std} or $-\xi_{std}$.

In later sections, we will glue two symplectic manifolds together along their boundaries, which are a lens space, using a contactomorphism. Thus we review contactomorphisms on lens spaces here. We denote by $\text{Cont}(L(p, q), \xi_{std})$ the group of coorientation preserving contactomorphisms of $L(p, q)$ with its standard contact structure.

Theorem 2.18 (Min [22]). *The contact mapping class group of $(L(p, q), \xi_{std})$ is*

$$\pi_0(\text{Cont}(L(p, q), \xi_{std})) = \begin{cases} \mathbb{Z}_2 & p \neq 2 \text{ and } q \equiv -1 \pmod{p}, \\ \mathbb{Z}_2 & q \not\equiv \pm 1 \pmod{p} \text{ and } q^2 \equiv 1 \pmod{p}, \\ 1 & \text{otherwise.} \end{cases}$$

The following is a direct corollary of Theorem 2.18.

Corollary 2.19. *Let ξ_{std} be a standard contact structure on $L(p^2, pq - 1)$.*

- (1) *The identity map*

$$id: (L(p^2, pq - 1), \xi_{std}) \rightarrow (L(p^2, pq - 1), \xi_{std})$$

is a unique coorientation preserving contactomorphism up to contact isotopy.

- (2) *There exists a unique coorientation reversing contactomorphism*

$$\tau: (L(p^2, pq - 1), \xi_{std}) \rightarrow (L(p^2, pq - 1), -\xi_{std})$$

up to contact isotopy. The diffeomorphism τ is defined on each of the Heegaard tori $S^1 \times D^2$ as $(\theta, z) \mapsto (-\theta, \bar{z})$ where we think of D^2 as the unit disk in \mathbb{C} .

Proof. Suppose $|p| > 2$. Then, $pq - 1 \not\equiv -1 \pmod{p^2}$ and $(pq - 1)^2 \not\equiv 1 \pmod{p^2}$, so $\pi_0(L(p^2, pq - 1), \xi_{std}) = 1$. If $|p| = 2$, then for any odd number q , $L(p^2, pq - 1) \cong L(4, 1)$ and $\pi_0(L(4, 1), \xi_{std}) = 1$. This completes the proof of the first statement.

It is well known (c.f. [14, 22]) that for any standard contact structure on a lens space, there exists a coorientation reversing contactomorphism τ . Suppose there is another coorientation reversing contactomorphism τ' . Then $\tau \circ (\tau')^{-1}$ is a coorientation preserving contactomorphism, and by the above argument, it is contact isotopic to the identity. Therefore, τ is contact isotopic to τ' and this completes the proof of the second statement. \square

3. HANDLEBODY CONSTRUCTION OF CLOSED SYMPLECTIC 4-MANIFOLDS

In this section, we will construct closed symplectic 4-manifolds with $b_2 = 1$ into which we can embed three of the $B_{p,q}$, and will show that they admit symplectic handlebody decompositions. In Section 3.1, we slightly modify Theorem 2.12 to create a symplectic cap and in Section 3.2, we study certain surgeries on torus knots in some contact lens spaces, which enable us to understand what contact structures we constructed a cap for in Theorem 3.1. Finally, in Section 3.3, we construct closed symplectic 4-manifolds for each Markov triple.

3.1. Construction of a small symplectic cap. Let (\mathcal{B}, π) be a (rational) open book decomposition supporting $(M, \xi_{\mathcal{B}})$. Suppose $\mathcal{B} = (K_1, \dots, K_m)$ is a (reference framed) link, and $\mathbf{n} = (n_1, \dots, n_m)$ is a set of integers that are greater than the page slopes of each binding component. Let $(\overline{\mathcal{B}}, \overline{\pi})$ be the mirror of (\mathcal{B}, π) supporting $(-M, \xi_{\overline{\mathcal{B}}})$. Here by the mirror of \mathcal{B} , we just mean \mathcal{B} thought of as sitting in M with its reversed orientation and $\overline{\pi}$ is the obvious projection $(-M \setminus \overline{\mathcal{B}}) \rightarrow S^1$. We denote the result of admissible transverse $-n_i$ -surgeries on every binding component by $(-M_{\overline{\mathcal{B}}}(-\mathbf{n}), \xi_{\overline{\mathcal{B}}}(-\mathbf{n}))$. Also recall that when we say (C, ω) is a symplectic cap for (M, ξ) , the orientation of M is opposite of the usual boundary orientation of C .

Theorem 3.1. *With the notations above, the cobordism W from M to $M_{\mathcal{B}}(\mathbf{n})$ obtained by attaching n_i -framed 2-handles to $[0, 1] \times M$ along on every $\{1\} \times K_i$ admits a symplectic structure ω that gives a strong symplectic cap for $(M, \xi_{\mathcal{B}}) \sqcup (-M_{\overline{\mathcal{B}}}(-\mathbf{n}), \xi_{\overline{\mathcal{B}}}(-\mathbf{n}))$.*

Proof. We will first show that \mathcal{B} is a nicely fibered link in $(M, \xi_{\mathcal{B}})$. First, take a contact form α of $\xi_{\mathcal{B}}$ and polar coordinates (r, θ, ϕ) near each binding component from Lemma 2.6. Then we choose the Reeb vector field R_α as our contact vector field in Definition 2.11 and directly calculate it to be

$$R_\alpha = A \frac{\partial}{\partial \theta} + B \frac{\partial}{\partial \phi}.$$

Since $d\alpha$ is a volume form of each page and $i_{R_\alpha} \alpha = 0$, clearly R_α is transverse to each page, which verifies the first bullet point of Definition 2.11. Also it is straightforward to verify the statements in the second bullet point. For the third bullet point, as in the proof

of Lemma 2.6, the characteristic foliation of a page is defined by the Liouville vector field so it points in towards the binding components.

Thus we can apply Theorem 2.12 to $([0, 1] \times M, d(e^t \alpha))$, a piece of the symplectization of (M, ξ) , to obtain a symplectic cap with two boundary components. We are now left to show that the contact manifold obtained on the upper boundary of the handle attachment is $(-M_{\overline{\mathcal{B}}}(-\mathbf{n}), \xi_{\overline{\mathcal{B}}}(-\mathbf{n}))$. Clearly the handle attachment gives a cobordism from M to $M_{\mathcal{B}}(\mathbf{n})$. Since we consider concave boundaries, we reverse the orientation of $M_{\mathcal{B}}(\mathbf{n})$ and obtain $-M_{\overline{\mathcal{B}}}(-\mathbf{n})$. Let \mathcal{B}^* be the surgery dual link of \mathcal{B} . The proof of [13, Theorem 1.2] and [13, Addendum 5.1] implies that the resulting contact structure is supported by $\overline{\mathcal{B}^*}$ and by Theorem 2.4, it is contactomorphic to $\xi_{\overline{\mathcal{B}}}(-\mathbf{n})$. \square

3.2. Non-loose torus knots in lens spaces. To utilize Theorem 3.1, we need to identify the resulting contact structure on $-M_{\overline{\mathcal{B}}}(-\mathbf{n})$, the manifold obtained by admissible transverse surgery along the binding of a (rational) open book decomposition. In general, it is not easy to describe this new contact structure in a more standard form, especially when the contact structure $\xi_{\overline{\mathcal{B}}}$ is overtwisted (which it frequently will be if $\xi_{\mathcal{B}}$ is tight). The main result of this section is Theorem 3.7, which makes such an identification in a special case.

We first characterize the contact structures on a lens space supported by a torus knot. Let $L(r, s)$ be a lens space for relatively prime integers r, s . Recall from Section 2.4 that a torus knot $T_{p,q}$ in $L(r, s)$ is a *positive* torus knot if q/p is clockwise of 0 and counterclockwise of $-r/s$ in the Farey graph, and a *negative* torus knot if q/p is clockwise of $-r/s$ and counterclockwise of 0 in the Farey graph. The following proposition is straightforward from [3, Theorem 1.8].

Proposition 3.2. *Let $T_{p,q}$ be a positive torus knot in $L(r, s)$ and $\xi_{p,q}$ be the contact structure on $L(r, s)$ supported by $T_{p,q}$. Then $\xi_{p,q}$ is a standard contact structure on $L(r, s)$.*

Next we consider negative torus knots. To do so, we require a few preliminary results.

Definition 3.3. Suppose (M, ξ) is an overtwisted contact 3-manifold. A Legendrian knot $L \subset (M, \xi)$ is called *non-loose* if $(M \setminus N, \xi|_{M \setminus N})$ is tight where N is a standard neighborhood of L . Similarly, a transverse knot $K \subset (M, \xi)$ is called *non-loose* if $(M \setminus K, \xi|_{M \setminus K})$ is tight.

In [10], non-loose torus knots in any contact structure on S^3 were classified. We can adapt the same method to describe the contact structure on a lens space supported by a negative torus knot in terms of decorated paths in the Farey graph.

Let P be a decorated path in the Farey graph for $(L(r, s), \xi)$. There are two important decorated paths we need to consider: *consistent paths* and *totally inconsistent paths*. A *consistent path* P is a decorated path $\{s_0, \dots, s_n\}$ where the signs of all edges are identical except for the first and the last ones. The signs of the two edges (s_0, s_1) and (s_{n-1}, s_n) are \circ . A *totally inconsistent path at p/q* is a decorated path P where all signs of the edges (s, s')

clockwise of p/q are positive (resp. negative) and all signs of the edges (s, s') counter-clockwise of p/q are negative (resp. positive) except for the first and last ones. The signs of the two edges are \circ . See Figure 7 for a totally inconsistent path at $-8/5$.

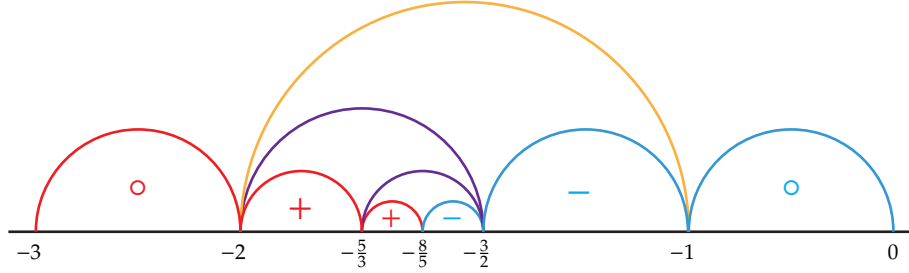


FIGURE 7. A decorated path in the Farey graph for the contact structure on $L(3, 1)$ supported by the rational open book decomposition $(T_{8,-5}, \pi)$.

Let $T_{p,q}$ be a torus knot in $L(r, s)$. Recall from Section 2.4 that $T_{p,q}$ is a simple closed curve on a Heegaard torus of $L(r, s)$. Thus there is a framing for $T_{p,q}$ induced from the Heegaard torus. We call it the *torus framing* of $T_{p,q}$. Also recall from Section 2.4 that $T_{p,q}$ is *trivial* if $|pr + qs| = 1$ or $|p| = 1$, and *nontrivial* otherwise.

Proposition 3.4. *Suppose $\xi_{p,q}$ is the contact structure on $L(r, s)$ supported by a negative torus knot $T_{p,q}$. Then it is overtwisted if $T_{p,q}$ is nontrivial. Further, $\xi_{p,q}$ may be described by a totally inconsistent path for $L(r, s)$ at q/p .*

Proof. Let N be a neighborhood of $T_{p,q}$ and define $C = L(r, s) \setminus N$. First we consider N as a standard neighborhood S_a of $T_{p,q}$ in $\xi_{p,q}$ for some $a \in \mathbb{Q}$ and let ξ_C be the restriction of $\xi_{p,q}$ to C . By Lemma 2.5, ξ_C is universally tight and we may assume that $a \in \mathbb{Q}$ is any slope less than the page slope. The torus knot $T_{p,q}$ sits on a Heegaard torus T of $L(r, s)$, and since $T_{p,q}$ is a negative torus knot, Lemma 2.7 tells us that the torus framing is less than the page slope so we can assume a is the slope corresponding to the torus framing. Now N is a neighborhood of a Legendrian knot L that is a Legendrian approximation of $T_{p,q}$, see [8, Section 2], and its contact framing agrees with the torus framing. We can smoothly perturb T so that L lies on T and perturb T again while fixing L so that it becomes convex with dividing slope q/p . Now T splits $L(r, s)$ into two solid tori S_1 and S_2 and hence the path describing the contact structure $\xi_{p,q}$ into two paths P_1 and P_2 . Since the core of both S_1 and S_2 are homotopically nontrivial in C , S_1 and S_2 unwrap in coverings of C . Thus the contact structures restricted to S_1 and S_2 should both be universally tight. This implies that each path only contains a single sign. Now there are two cases to consider. First, both paths P_1 and P_2 have the same sign. In this case, the decorated path for $L(r, s)$ is a totally consistent path. In [10, Lemma 3.16], it was shown that adding Giroux torsion to C in the totally consistent setting always produces an overtwisted contact structure. (In [10] only the case of S^3 was considered, but the proof only used a thickened torus containing $T_{p,q}$ and so applies to lens spaces as well.) By Lemma 2.5, adding Giroux

torsion to the complement of $T_{p,q}$ in $\xi_{p,q}$ gives a tight contact manifold. Thus the signs in P_1 and P_2 must be opposite and the path describing $\xi_{p,q}$ is totally inconsistent at p/q .

Since $T_{p,q}$ is nontrivial, the decorated path is not minimal and we can shorten the path by merging two edges $((q/p)^a, q/p)$ and $(q/p, (q/p)^c)$. (See Section 2.7 for notation.) However, since the two edges had different signs, $\xi_{p,q}$ is overtwisted by Theorem 2.16. \square

Now we return to the the contact manifolds obtained by surgery on torus knots. We first study a certain surgery on $T^2 \times I$, for which we require following amusing lemma.

Lemma 3.5. *Let P be a pair of pants. Dehn filling any boundary component of $P \times S^1$ along the curve $\{p\} \times S^1$ results in a connected sum of two solid tori, and this homeomorphism sends $\{p\} \times S^1$ to the meridians of the solid tori.*

Proof. Let T be the boundary component of $P \times S^1$ that is filled and γ be an essential arc on $P \times \{x\}$ such that $\partial\gamma \subset T$. Then $A = \gamma \times S^1$ is an essential annulus in $P \times S^1$ and each boundary component bounds a disk after the Dehn filling. The union of the two disks and A is an essential sphere. We cut the manifold along the sphere and obtain two copies of $D^2 \times S^1 \setminus B^3$. Therefore, the result of Dehn filling should be a connected sum of two solid tori. Each $\{p\} \times S^1$ bounds a disk and hence becomes a meridian. \square

We now consider a similar situation in the contact geometry setting.

Lemma 3.6. *Let K be a slope 0 curve in $T^2 \times \{0\}$ in the contact structure on $T^2 \times [-1, 1]$ given by the union of basic slices $B_{\pm}(-1, 0) \cup B_{\mp}(0, \infty)$. There is a non-loose Legendrian representative L of K such that the contact framing is 1 larger than the torus framing. Moreover, Legendrian surgery on L yields a connected sum of two tight solid tori $S^0(-1) \# S_0(\infty)$.*

Proof. We first show that the claimed L exists. Notice that the basic slice $B_{\mp}(0, \infty)$ can be written as the union of two basic slices, $B_{\mp}(0, 1)$ and $B_{\mp}(1, \infty)$. The union $B_{\pm}(-1, 0) \cup B_{\mp}(0, 1)$ is called a length 2 balanced continued fraction block with central slope 0. In [5, Theorem 1.11] it was shown that inside such a thickened torus there is a unique Legendrian knot L isotopic to the slope 0 curve with framing one larger than the torus framing. Below we will see Legendrian surgery on L yields a tight contact structure and thus L is non-loose.

Since Legendrian surgery on L is a topological 0-surgery on K , Lemma 3.5 shows that the resulting manifold is a connected sum of two solid tori such that the 0-slope curves on $T^2 \times \{-1, 1\}$ become the meridians. It remains to show the contact structure on each component is tight. Let $M = B_{\pm}(-1, 0) \cup B_{\mp}(0, \infty) \setminus N$ where N is a standard neighborhood of L . Take a properly embedded essential annulus A in M where each boundary component of A is a 0-slope curve on ∂N . We cut M along A and obtain two tight $T^2 \times I$ layers after edge rounding. Notice that these layers are minimally twisting. Now, Legendrian surgery on L in $B_{\pm}(-1, 0) \cup B_{\mp}(0, \infty)$ is equivalent to the contact Dehn fillings on each $T^2 \times I$ layer using a 0-slope curve and then remove a Darboux ball in each and glue

them together along the convex spheres. Since both layers are minimally twisting, each solid torus is tight so the result of Legendrian surgery should be $S_0(-1) \# S_0(\infty)$. \square

Let $T_{p,q}$ be a torus knot in $L(r, s)$ and $\xi_{p,q}$ be the contact structure on $L(r, s)$ supported by $T_{p,q}$. When we perform a surgery on $T_{p,q}$, we call it a *torus framing surgery* if the surgery coefficient is the torus framing. Recall from Section 2.7 that $q'/p' = (q/p)^c$ is the largest rational number satisfying $pq' - p'q = -1$ and $q''/p'' = (p/p)^a$ is the smallest rational number satisfying $pq'' - p''q = 1$.

Theorem 3.7. *The torus framing admissible transverse surgery on a non-trivial negative torus knot $T_{p,q}$ in $(L(r, s), \xi_{p,q})$ results in a connected sum of standard contact structures on $L(p, -q)$ and $L(ps + qr, \bar{p}s + \bar{q}r)$ for any integers \bar{p} and \bar{q} satisfying $p\bar{q} - \bar{p}q = -1$.*

For example, the torus framing admissible transverse surgery on $T_{5,-8}$ in $(L(3, 1), \xi_{5,-8})$ yields a connected sum of standard contact structures on $L(8, 5)$ and $L(7, 3)$. See Figure 8.

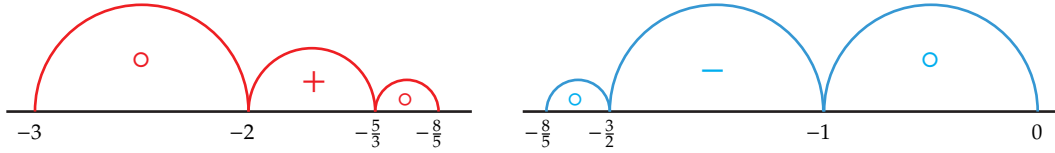


FIGURE 8. Decorated paths in the Farey graph for the standard contact structures on $L(7, 3)$ and $L(8, 5)$.

Proof. We first show that the torus framing admissible transverse surgery on $T_{p,q}$ is equivalent to Legendrian surgery on one of its Legendrian approximations. By Lemma 2.5, there is a neighborhood S_a of $T_{p,q}$ in $(L(r, s), \xi_{p,q})$ where a is any number less than the page slope. Since $T_{p,q}$ is a non-trivial negative torus knot, Lemma 2.7 says the torus framing plus one is less than the page slope so we can assume that S_a has slope one larger than the torus framing. Thus as in the proof of Proposition 3.4 we can assume that S_a is a standard neighborhood of a Legendrian knot L with contact framing one larger than the torus framing and $T_{p,q}$ is the transverse push-off of L . The proof of Proposition 2.1 shows that torus framing admissible surgery on $T_{p,q}$ is the same as Legendrian surgery on L .

Since by Proposition 3.4 the decorated path describing the contact structure $\xi_{p,q}$ is totally inconsistent at q/p we know that inside of $L(r, s)$ we see the union of two basic slices

$$B_{\pm}(p''/q'', p/q) \cup B_{\mp}(p/q, p'/q').$$

Now we change the coordinates using the following map

$$\phi = \begin{pmatrix} p' & -q' \\ -p & q \end{pmatrix}.$$

Then ϕ sends $p/q \mapsto 0$, $p'/q' \mapsto \infty$ and $p''/q'' \mapsto -1$. As in the proof of Lemma 3.6 we see there is a Legendrian knot L realizing a 0 sloped curve with contact framing one larger than the torus framing. Thus $\phi(L)$ is now a Legendrian knot in $B_{\pm}(-1, 0) \cup B_{\mp}(0, \infty)$ such that the contact framing is one larger than the torus framing and [5, Theorem 1.11] says that $\phi(L)$ is the Legendrian in Lemma 3.6. Now we apply Lemma 3.6 and obtain a connected sum of two tight solid tori. Pulling back this contact manifold using ϕ^{-1} , we obtain a connected sum of tight solid tori with meridian slope p/q . Thus the result of surgery is a connected sum of two lens spaces such that one has meridian slopes p/q and 0, and the other one has meridian slopes $-r/s$ and p/q . The first lens space is clearly $L(p, -q)$, and by changing the coordinates using the following map

$$\psi = \begin{pmatrix} \bar{p} & -\bar{q} \\ -p & q \end{pmatrix}$$

sending $p/q \mapsto 0$ and $-r/s \mapsto (ps + qr)/(-\bar{p}s - \bar{q}r)$, we can see the second lens space should be $L(ps + qr, \bar{p}s + \bar{q}r)$. Thus we obtain

$$L(p, -q) \# L(ps + qr, \bar{p}s + \bar{q}r).$$

Finally, since the signs of the edges in the decorated path clockwise of p/q are the same, the contact structure on $L(p, -q)$ is universally tight by Theorem 2.16 so it is standard. Similarly, the contact structure on $L(ps + qr, \bar{p}s + \bar{q}r)$ is also standard. \square

3.3. Symplectic pants cobordisms for Markov triples. In this section we will build the symplectic cap for three lens spaces coming from a Markov triple. To identify these lens spaces we need a preliminary result about Markov triples.

Proposition 3.8. *For any Markov triple (p_1, p_2, p_3) , there exists a triple of positive integers (q_1, q_2, q_3) satisfying the equations*

- (1) $p_3^2 = (p_1q_1 - 1)p_2^2 + p_1^2(p_2q_2 - 1)$
- (2) $p_3q_3 - 1 = p_2^2q_1^2 + (p_1q_1 + 1)(p_2q_2 - 1)$
- (3) $q_i = \pm 3p_j/p_k \pmod{p_i}$
- (4) $q_1 \leq 0$

where (i, j, k) is a permutation of 1, 2, 3.

Proof. Pick two integers $x \geq 0$ and $y \leq 0$ satisfying $p_1x + p_2y = 1$. Then define

$$\begin{aligned} q_1 &:= 3p_3y \\ q_2 &:= 3p_3x \\ q_3 &:= -3p_1y + 3p_2x + 9p_2p_3y \end{aligned}$$

The fact that the choices of q_1 and q_2 satisfy the third condition is immediate. We will show that they satisfy the first condition.

$$\begin{aligned} (p_1q_1 - 1)p_2^2 + p_1^2(p_2q_2 - 1) &= 3p_1p_2^2p_3y + 3p_1^2p_2p_3x - p_1^2 - p_2^2 \\ &= 3p_1p_2p_3 - p_1^2 - p_2^2 \\ &= p_3^2 \end{aligned}$$

The definition of q_3 is chosen so that the second condition is satisfied, as can easily be checked by noting that $p_1q_2 + p_2q_1 = 3p_3$. To show that it satisfies the third condition, it's enough to prove that $p_1y - p_2x = 3p_2/p_1 \pmod{p_3}$. This follows from elementary number theory and properties of Markov triples and their characteristic numbers. The reader can refer to Chapter 2 in [2] for similar computations. The fourth condition is immediate from $y \leq 0$. \square

Definition 3.9. Let (p_1, p_2, p_3) be a Markov triple and (q_1, q_2, q_3) be a triple of integers from Proposition 3.8. We call a compact symplectic 4-manifold (P, ω_P) a (concave) symplectic pants cobordism for (p_1, p_2, p_3) if $b_2(P) = 1$ and (P, ω_P) is a strong symplectic cap with three concave boundary components

$$\bigsqcup_{i=1}^3 L(p_i^2, p_iq_i - 1).$$

Remark 3.10. Notice that the orientations of concave boundary components are the opposite of the ordinary boundary orientations. Thus a symplectic pants cobordism is a smooth cobordism from $L(p_3^2, p_3q_3 - 1)$ to $L(-p_1^2, p_1q_1 - 1) \sqcup L(-p_2^2, p_2q_2 - 1)$.

Theorem 3.11. For any Markov triple (p_1, p_2, p_3) , there exists a symplectic pants cobordism (P, ω_P) for (p_1, p_2, p_3) such that the induced contact structure on each boundary component is standard. Further, (P, ω_P) admits a (relative) symplectic handlebody decomposition consisting of one convex-concave 2-handle and one concave 3-handle attached to $L(p_3^2, p_3q_3 - 1)$.

Proof. Let K be a $(-p_1q_1 - 1, p_1^2)$ -torus knot in $(L(p_3^2, p_3q_3 - 1), \xi_{std})$. We first claim that K is a positive torus knot in $L(p_3^2, p_3q_3 - 1)$. First, by Proposition 3.8 we know $q_1 \leq 0$. Assume $q_1 = 0$. Then according to the proof of Proposition 3.8, we have $x = 1$ and $y = 0$, which implies that $p_1 = 1$ and $q_3 = 3p_2$. Thus the defining equation $p_1^2 + p_2^2 + p_3^2 = 3p_1p_2p_3$ gives us $p_3^2 = 2p_2p_3 - 1 - p_2^2$ and so we have

$$\frac{p_1^2}{-p_1q_1 - 1} = -1 < -\frac{p_3^2}{p_3q_3 - 1} = -\frac{p_3^2}{3p_2p_3 - 1} < 0$$

and K is a positive torus knot by the definition in Section 2.4. Now assume $q_1 < 0$. There are two cases we need to consider. First, suppose $q_3 > 0$. Then we have

$$-\frac{p_3^2}{p_3q_3 - 1} < 0 < \frac{p_1^2}{-p_1q_1 - 1}$$

so K is a positive torus knot. Next, suppose $q_3 < 0$. Then one can see that $0 > -p_2^2$ implies that $p_1^2(p_2^2q_1^2 + (p_1q_1 + 1)(p_2q_2 - 1)) > ((p_1q_1 - 1)p_2^2 + p_1^2(p_2q_2 - 1))(p_1q_1 + 1)$ and using Proposition 3.8 that inequality implies that $p_1^2(p_3q_3 - 1) > p_3^2(p_1q_1 + 1)$, which of course gives

$$\frac{p_1^2}{-p_1q_1 - 1} < -\frac{p_3^2}{p_3q_3 - 1}$$

Combining with the fact $p_1^2/(-p_1q_1 - 1) > 0$, we can conclude that K is a positive torus knot.

Therefore, the torus framing of K is greater than the page slope by Lemma 2.7. Also by Theorem 3.2, K supports a standard contact structure. Thus K satisfies the hypothesis of Theorem 3.1, so we obtain a strong symplectic cap (C, ω_C) by attaching a convex-concave 2-handle along K with the torus framing. Recall that we orient the concave boundary of a symplectic cap as the opposite of the ordinary boundary orientation, so the resulting contact 3-manifold is the result of the torus framing admissible transverse surgery on a negative torus knot \bar{K} , the $(p_1q_1 + 1, p_1^2)$ -torus knot supporting the contact structure $\xi_{p_1q_1+1, p_1^2}$ on $L(-p_3^2, p_3q_3 - 1)$. It is straightforward to check

$$p_1^2(-q_1^2) - (p_1q_1 - 1)(p_1q_1 + 1) = 1.$$

Therefore by Theorem 3.7, the result of the surgery is a connected sum of standard contact structures on

$$L(p_1^2, -p_1q_1 - 1) \# L(p_1^2(p_3q_3 - 1) + (p_1q_1 + 1)(-p_3^2), (p_1q_1 - 1)(p_3q_3 - 1) - q_1^2(-p_3^2)).$$

Since $(-p_1q_1 - 1)(p_1q_1 - 1) \equiv 1 \pmod{p_1^2}$, the first lens space is diffeomorphic to $L(p_1^2, p_1q_1 - 1)$. Also by Proposition 3.8, we have

$$\begin{pmatrix} -p_1q_1 - 1 & q_1^2 \\ -p_1^2 & p_1q_1 - 1 \end{pmatrix} \begin{pmatrix} 1 - p_2q_2 \\ p_2^2 \end{pmatrix} = \begin{pmatrix} p_2^2q_1^2 + (p_1q_1 + 1)(p_2q_2 - 1) \\ p_2^2(p_1q_1 - 1) + p_1^2(p_2q_2 - 1) \end{pmatrix} = \begin{pmatrix} p_3q_3 - 1 \\ p_3^2 \end{pmatrix},$$

and this implies

$$\begin{pmatrix} p_1q_1 - 1 & -q_1^2 \\ p_1^2 & -p_1q_1 - 1 \end{pmatrix} \begin{pmatrix} p_3q_3 - 1 \\ p_3^2 \end{pmatrix} = \begin{pmatrix} -q_1^2p_3^2 + (p_1q_1 - 1)(p_3q_3 - 1) \\ -(p_1q_1 + 1)p_3^2 - p_1^2(1 - p_3q_3) \end{pmatrix} = \begin{pmatrix} 1 - p_2q_2 \\ p_2^2 \end{pmatrix},$$

Thus the second lens space is $L(p_2^2, p_2q_2 - 1)$.

Separately, observe that we can attach a Weinstein 1-handle to (a part of the symplectizations of)

$$(L(p_1^2, p_1q_1 - 1), \xi_{std}) \text{ and } (L(p_2^2, p_2q_2 - 1), \xi_{std})$$

and obtain a Weinstein cobordism (W, ω_W) from

$$(L(p_1^2, p_1q_1 - 1), \xi_{std}) \sqcup (L(p_2^2, p_2q_2 - 1), \xi_{std})$$

to

$$(L(p_1^2, p_1q_1 - 1) \# L(p_2^2, p_2q_2 - 1), \xi_{std} \# \xi_{std}).$$

Now we have a symplectic cap (C, ω_C) and a Weinstein cobordism (W, ω_W) . The concave boundary of (C, ω_C) and the convex boundary of (W, ω_W) are contactomorphic, so we can glue (C, ω_C) and (W, ω_W) together along $L(p_2^2, p_2q_2 - 1) \# L(p_3^2, p_3q_3 - 1)$ and obtain the desired pants cobordism. Since a Weinstein 1-handle can be considered a concave 3-handle when turned upside down, we can obtain the pants cobordism by attaching a convex-concave 2-handle and a concave 3-handle to $L(p_3^2, p_3q_3 - 1)$. See Figure 9 for a schematic picture for the pants cobordism. \square

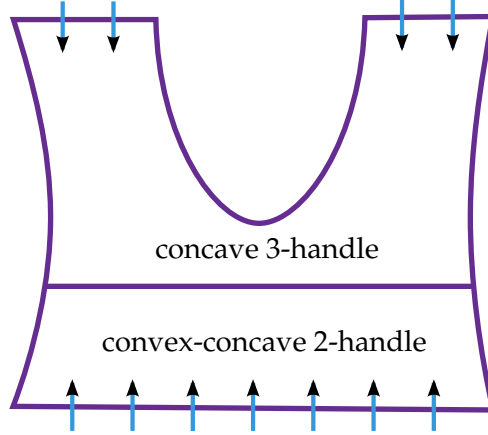


FIGURE 9. A schematic picture for a concave pants cobordism.

Let (p_1, p_2, p_3) be a Markov triple and (P, ω_P) is a (concave) symplectic pants cobordism for (p_1, p_2, p_3) from Theorem 3.11. Since the induced contact structure on each concave boundary component of (P, ω) is standard, we can glue three Weinstein B_{p_i, q_i} along the boundary components and obtain a closed symplectic 4-manifold $(X_{p_1, p_2, p_3}, \omega_{p_1, p_2, p_3})$. This construction is unique up to diffeomorphism since any contactomorphism of a standard contact structure on $L(p_i^2, p_iq_i - 1)$ extends to a diffeomorphism of B_{p_i, q_i} according to Remark 2.15. From the handlebody viewpoint, we consider this as starting from Weinstein B_{p_3, q_3} , attaching a pants cobordism (P, ω_P) (equivalently attaching a convex-concave 2 handle and a concave 3-handle, see Theorem 3.11). After that, we attach the upside down Weinstein B_{p_1, q_1} and B_{p_2, q_2} to each concave boundary component of the pants cobordism. Since we completely understand the Weinstein handlebody structure of each B_{p_i, q_i} , this gives a symplectic handlebody decomposition of $(X_{p_1, p_2, p_3}, \omega_{p_1, p_2, p_3})$.

The next proposition summarizes the discussion above.

Proposition 3.12. *For any Markov triple (p_1, p_2, p_3) , there exists a closed symplectic 4-manifold $(X_{p_1, p_2, p_3}, \omega_{p_1, p_2, p_3})$ built from the symplectic pants cobordism for (p_1, p_2, p_3) and B_{p_i, q_i} . Moreover, $(X_{p_1, p_2, p_3}, \omega_{p_1, p_2, p_3})$ admits a symplectic handlebody decomposition consisting of a convex 0-handle, a convex 1-handle, a convex 2-handle, a convex-concave 2-handle, two concave 2-handles, three concave 3-handles, and two concave 4-handles.*

Currently, it is not clear that X_{p_1, p_2, p_3} is \mathbb{CP}^2 or that the symplectic structure ω_{p_1, p_2, p_3} is deformation equivalent to a symplectic structure on \mathbb{CP}^2 . In the following two sections, we will show that X_{p_1, p_2, p_3} is indeed \mathbb{CP}^2 and that ω_{p_1, p_2, p_3} is deformation equivalent to the standard symplectic structure on \mathbb{CP}^2 .

4. FROM SYMPLECTIC HANDLEBODIES TO HORIZONTAL DECOMPOSITIONS

In order to exhibit explicitly the symplectic structure on the manifolds X_{p_1, p_2, p_3} in Section 3, it is convenient to use the pants construction outlined in Section 3.3. However, in order to identify these manifolds as \mathbb{CP}^2 , it is convenient to use a construction known as *horizontal handle decompositions*, introduced in recent work of Lisca and Parma, [20]. In Section 4.1, we will introduce horizontal handle decompositions and recall the relevant results from [20, 21]. In Section 4.2, we will convert our construction from Section 3.3 into a horizontal handle diagram as shown in Figure 13. This conversion will be used to prove Theorem 4.6 that identifies X_{p_1, p_2, p_3} with \mathbb{CP}^2 in Section 4.3, which completes our proof of Theorem 1.1 and explicitly symplectically embeds three rational homology balls associated to Markov triples into \mathbb{CP}^2 .

4.1. Horizontal handle decompositions. Horizontal handle decompositions were developed by Lisca and Parma in [20]. The following treatment will be brisk; for more details, see [20].

Let H be a handle decomposition of a closed 4-manifold X . By a standard argument, H can be assumed to have a unique 0-handle and a unique 4-handle. Let H_1 denote the sub-handlebody consisting of the 0- and 1-handles.

Definition 4.1. A handle decomposition H is *horizontal* with genus g if $\partial(H_1)$ admits a genus g Heegaard splitting surface Σ such that

- (1) There is some order $\{h_i : i \in \mathbb{N}\}$ on the set of 2-handles of H such that the 2-handles can be isotoped in ∂H_1 so that in some neighborhood $\Sigma \times [0, 1]$ of Σ , the attaching sphere of h_i is a non-separating simple closed curve on $\Sigma \times \{1 - 1/i\}$.
- (2) each 2-handle framing f_i is equal to $f_\Sigma \pm 1$ where f_Σ is the framing induced by Σ .

The requirements about Σ and the 2-handle framings in the definition of a horizontal handle decomposition cause the 2-handle attachments to naturally modify a Heegaard splitting of the boundary. More precisely, let H be a horizontal handle decomposition and let H_1^j denote the sub-handlebody of H consisting of H_1 together with h_1, \dots, h_j , the first j 2-handles. Lemma 2.14 guarantees that for all j , ∂H_1^j inherits a natural genus g Heegaard splitting. The theory of horizontal handle diagrams is thus particularly helpful to demonstrate disjoint embeddings of a collection of 3-manifolds with bounded Heegaard genus into a 4-manifold.

Lisca and Parma utilize this theory to give smooth embeddings of collections of lens spaces into \mathbb{CP}^2 . They also give classifications of the smooth 4-manifolds realized by horizontal decompositions with small genus. We will use one of their classification results.

For the statement, recall that an essential simple closed curve on T^2 can be written as $\gamma = q\lambda_U + p\mu_U$ where μ_U and λ_U are curves on T^2 that form a symplectic basis of $H_1(T^2)$.

Theorem 4.2 (Lisca–Parma [21]). *Let X be a closed oriented 4-manifold with a horizontal decomposition of genus one having one 0-handle, one 1-handle, three 2-handles, one 3-handle, and one 4-handle. Suppose that the 2-handles are attached along essential simple closed curves γ_1 , γ_2 , and γ_3 such that each has framing -1 relative to the surface framing. Let $x_1 := \gamma_2 \cdot \gamma_3$, $x_2 := \gamma_1 \cdot \gamma_3$, and $x_3 := \gamma_1 \cdot \gamma_2$. If $(x_1, x_2, x_3) \neq (0, 0, 0)$ and $x_1^2 + x_2^2 + x_3^2 = x_1x_2x_3$, then X is diffeomorphic to \mathbb{CP}^2 .*

To prove Theorem 4.6 that identifies X_{p_1, p_2, p_3} with \mathbb{CP}^2 , we will show in Section 4.2 that the symplectic 4-manifolds $(X_{p_1, p_2, p_3}, \omega_{p_1, p_2, p_3})$ we constructed in Section 3.3 in fact admit a horizontal handle decompositions which have the form in Theorem 4.2. The conclusion that our symplectic manifolds are in fact diffeomorphic to \mathbb{CP}^2 then follows from Theorem 4.2.

4.2. Converting pants to horizontal handles. In order to recognize the closed symplectic 4-manifolds we built in Proposition 3.12, we would like to draw an explicit horizontal handle diagrams of these manifolds, and then identify it using Theorem 4.2. When we built the symplectic pants cobordism in Theorem 3.11, the pants cobordism is described by attaching a 2-handle to a lens space; the resulting top boundary is a connected sum of lens spaces. We will find it convenient here to take the dual perspective. We begin in Proposition 4.3 by describing a 2-handle attachment to $B_{p_1, q_1} \natural B_{p_2, q_2}$ which results in a 4-manifold C with $\partial C = L(-p_3^2, p_3q_3 - 1)$. Then in Proposition 4.4 we show that this 2-handle cobordism from $L(p_1^2, p_1q_1 - 1) \# L(p_2^2, p_2q_2 - 1)$ to $L(-p_3^2, p_3q_3 - 1)$ is indeed the pants cobordism from Theorem 3.11 turned upside down. Finally, in Proposition 4.5 we give a handle diagram for the result of attaching B_{p_3, q_3} to C ; this final handle diagram describes the closed manifold X_{p_1, p_2, p_3} of Proposition 3.12. We will then prove Theorem 4.6 by applying Theorem 4.2 to our final horizontal handle diagram.

Proposition 4.3. *For pairs of integers (p_i, q_i) satisfying the conditions in Proposition 3.8, when a 2-handle is attached to the boundary connect sum $B_{p_1, q_1} \natural B_{p_2, q_2}$ with the attaching sphere and framing demonstrated in yellow in Figure 10, we obtain the 4-manifold given in Figure 12, which has boundary $L(-p_3^2, p_3q_3 - 1)$.*

Proof. Figure 10, 11, and 12 gives the 4-manifold diffeomorphism claimed.

From Figure 10 to the left hand side of Figure 11, we cancel one pair of 1- and 2-handles, and convert from a standard handle diagram to explicitly drawing the attaching spheres of the 2-handles in $S^1 \times S^2$. From the left hand side to the right hand side of Figure 11, we isotope the attaching spheres in $S^1 \times S^2$. From the right frame of Figure 11 to Figure 12, we convert back into a standard dotted circle notation.

That the boundary of Figure 12 is a lens space follows from Lemma 2.14. To compute which lens space, we use the method we set up in Remark 2.15. In the proof of

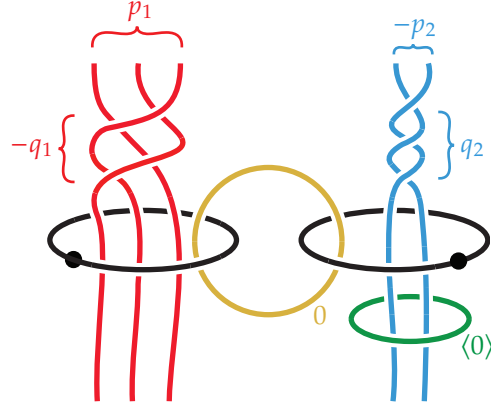


FIGURE 10. The boundary sum $B_{p_1, q_1} \natural B_{p_2, q_2}$ with a 2-handle attached. All red and blue 2-handles are -1 framed with respect to the torus framing. Angled brackets denote a framing we are watching, not an attaching instruction.

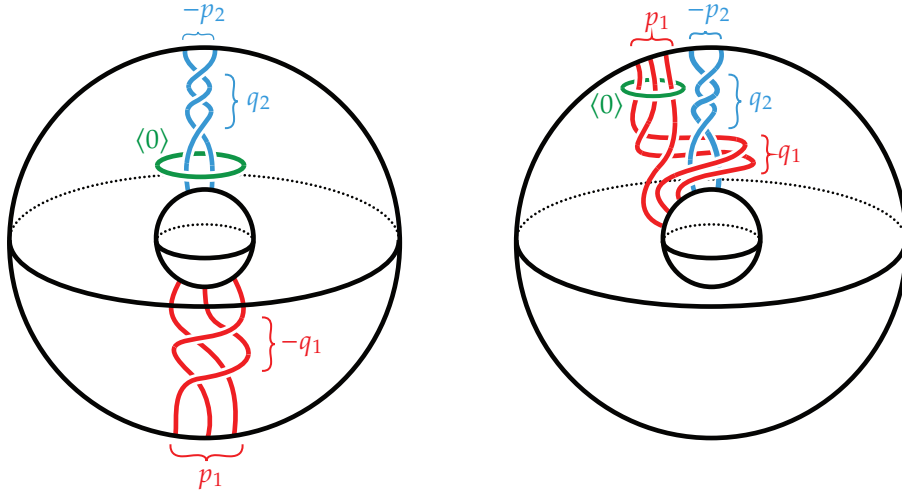


FIGURE 11. Attaching spheres of 2-handles in $S^1 \times S^2$. All red and blue 2-handles are -1 framed with respect to the torus framing. Angled brackets denote a framing we are watching, not an attaching instruction.

Lemma 2.13 we already computed that the result of pushing the longitude, $\begin{pmatrix} 1 \\ 0 \end{pmatrix}$, of black curve past the blue surgery curve is $\begin{pmatrix} 1 - p_2 q_2 \\ p_2^2 \end{pmatrix}$. As in Remark 2.15, we compute that subsequently pushing past red surgery curve gives

$$\begin{pmatrix} 1 + p_1 q_1 & -q_1^2 \\ p_1^2 & 1 - p_1 q_1 \end{pmatrix} \begin{pmatrix} 1 - p_2 q_2 \\ p_2^2 \end{pmatrix} = \begin{pmatrix} -p_2^2 q_1^2 - (p_1 q_1 + 1)(p_2 q_2 - 1) \\ p_1^2(1 - p_2 q_2) + p_2^2(1 - p_1 q_1) \end{pmatrix} = \begin{pmatrix} -(p_3 q_3 - 1) \\ -p_3^2 \end{pmatrix},$$

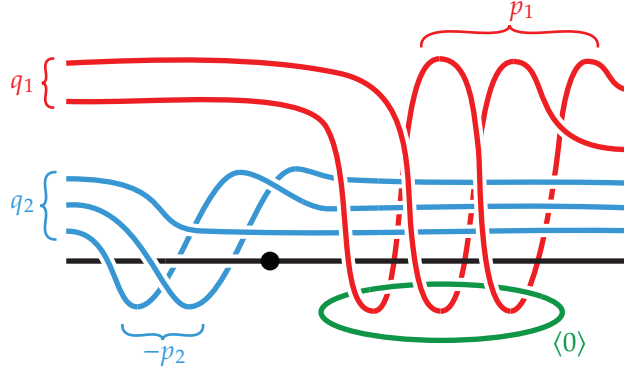


FIGURE 12. All red and blue 2-handles are -1 framed with respect to the torus framing. Angled brackets denote a framing we are watching, not an attaching instruction.

where the last equality comes from Proposition 3.8. \square

Let W_{p_1, p_2, q_1, q_2} denotes this 1- and (yellow) 2-handle cobordism from $L(p_1, q_1) \sqcup L(p_2, q_2)$ to $L(-p_3^2, p_3 q_3 - 1)$ shown in Figure 10.

Proposition 4.4. *If the pairs of integers (p_i, q_i) satisfy the equations in Proposition 3.8, then W_{p_1, p_2, q_1, q_2} is diffeomorphic to the pants cobordism from Theorem 3.11.*

Proof. To prove this, it suffices to locate the belt sphere of the 2-handle of W_{p_1, p_2, q_1, q_2} in $L(-p_3^2, p_3 q_3 - 1)$ and show that this agrees with the framed 2-handle described in Theorem 3.11.

We have exhibited the belt sphere of the yellow 2-handle of W_{p_1, p_2, q_1, q_2} in Figure 10 in green. The cocore disk 0-frames the belt sphere. To conclude we must identify this green curve in $L(-p_3^2, p_3 q_3 - 1)$. To do this, observe that in Figure 12 we can think of this belt sphere as living in the embedded torus in $L(-p_3^2, p_3 q_3 - 1)$ which is located between the blue and the red surgery curves; in this torus the surface framing agrees with the 0-framing. Then to identify this framed belt sphere in the (outermost) Heegaard torus for $L(-p_3^2, p_3 q_3 - 1)$, we simply must push it past the red surgery curve, and the new framing will be the new surface framing. As in the proof of Proposition 4.3, we compute

$$\begin{pmatrix} 1 + p_1 q_1 & -q_1^2 \\ p_1^2 & 1 - p_1 q_1 \end{pmatrix} \begin{pmatrix} 1 \\ 0 \end{pmatrix} = \begin{pmatrix} p_1 q_1 + 1 \\ p_1^2 \end{pmatrix}$$

which implies that the belt sphere is the $(p_1 q_1 + 1, p_1^2)$ -torus knot in $L(-p_3^2, p_3 q_3 - 1)$ and this completes the proof. \square

Proposition 4.5. *If the pairs of integers (p_i, q_i) satisfy the equations in Proposition 3.8, then the 4-manifold presented in Figure 13 is orientation preserving diffeomorphic to X_{p_1, p_2, p_3} .*

Proof. We have demonstrated already that there is an orientation preserving diffeomorphism from the handle diagram H in Figure 12 to the codimension 0 submanifold of

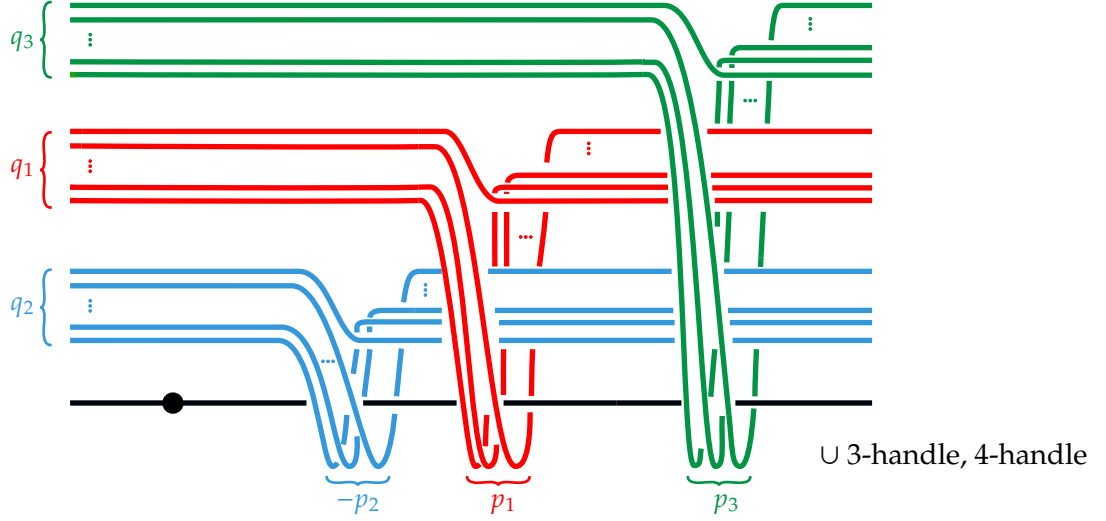


FIGURE 13. Horizontal handle decomposition of X_{p_1, p_2, p_3} . All three 2-handles are -1 framed with respect to the torus framing.

X_{p_1, p_2, p_3} obtained by removing the bottom rational ball, $B(p_3, q_3)$. So it remains to demonstrate that adding the additional handles in Figure 13 to H (i.e. the green 2-handle, and the 3- and 4-handle) corresponds exactly to regluing the rational ball $B(p_3, q_3)$.

Observe (say in Figure 4) that the 0-framed cocore of the 2-handle of $B(p_3, q_3)$ is the 1-framed $-p_3/q_3$ curve on the Heegaard torus for $L(p_3^2, p_3q_3 - 1)$. Then, to get a handle diagram of $B(p_3, q_3)$ upside down, we must attach a (-1) -framed 2-handle to $L(-p_3^2, p_3q_3 - 1) \times I$ along the p_3/q_3 curve on the Heegaard torus. Since this is exactly the way the green 2-handle is attached to H , we see that the 4-manifold presented in Figure 13 is orientation preserving diffeomorphic to X_{p_1, p_2, p_3} . \square

4.3. Symplectic embeddings of rational homology balls into \mathbb{CP}^2 . In Section 3.3, we constructed a closed symplectic 4-manifold $(X_{p_1, p_2, p_3}, \omega_{p_1, p_2, p_3})$ for each Markov triple (p_1, p_2, p_3) and in Section 4.2, we showed that X_{p_1, p_2, p_3} admits a genus one horizontal handlebody decomposition. Let ω_{std} be the standard symplectic structure on \mathbb{CP}^2 . We now show that it is immediate from Theorem 4.2 and the result of Taubes [25] that our manifold is the standard symplectic \mathbb{CP}^2 (after scaling the symplectic form).

Theorem 4.6. *The manifold $(X_{p_1, p_2, p_3}, \omega_{p_1, p_2, p_3})$ is deformation equivalent to $(\mathbb{CP}^2, \omega_{std})$.*

Proof. By Proposition 4.5, we know X_{p_1, p_2, p_3} is diffeomorphic to the closed 4-manifold shown in Figure 13. With the notations in Theorem 4.2, we have

$$\gamma_1 = -p_2\mu_U + q_2\lambda_U, \quad \gamma_2 = p_1\mu_U + q_1\lambda_U, \quad \gamma_3 = p_3\mu_U + q_3\lambda_U.$$

We also have

$$\begin{aligned} x_1 &= \gamma_2 \cdot \gamma_3 = p_1 q_3 - p_3 q_1, \\ x_2 &= \gamma_1 \cdot \gamma_3 = -p_2 q_3 - p_3 q_2, \\ x_3 &= \gamma_1 \cdot \gamma_2 = -p_2 q_1 - p_1 q_2. \end{aligned}$$

Using Proposition 3.8 one can show (through a non-trivial computation, carried out with the help of Mathematica) that the x_i satisfy the hypothesis in Theorem 4.2, and so it is immediate that X_{p_1, p_2, p_3} is diffeomorphic to \mathbb{CP}^2 . According to the result of Taubes [25, Theorem 0.3], there exists a unique symplectic structure on \mathbb{CP}^2 up to symplectic deformation. Thus $(X_{p_1, p_2, p_3}, \omega_{p_1, p_2, p_3})$ is symplectomorphic to $(\mathbb{CP}^2, \omega_{std})$ after scaling ω_{p_1, p_2, p_3} . \square

Remark 4.7. In Section 5, we will exhibit two more proofs of Theorem 4.6 using almost toric geometry.

Proof of Theorem 1.1. By Proposition 3.12, we know that $(X_{p_1, p_2, p_3}, \omega_{p_1, p_2, p_3})$ was built from B_{p_3, q_3} , which consists of convex (Weinstein) 0-, 1-, 2-handles, by attaching a convex-concave 2-handle, followed by gluing $B_{p_1, q_1} \natural B_{p_2, q_2}$ together along boundary. Here we consider $B_{p_1, q_1} \natural B_{p_2, q_2}$ as an upside down Weinstein domain. Thus $(X_{p_1, p_2, p_3}, \omega_{p_1, p_2, p_3})$ consists of a convex 0-handle, a convex 1-handle, a convex 2-handle, a convex-concave 2-handle, two concave 2-handles, three concave 3-handles, and two concave 4-handles. Combining with Theorem 4.6, this provides a symplectic handlebody decomposition of $(\mathbb{CP}^2, \omega_{std})$ in which we explicitly see embeddings of the rational homology balls B_{p_i, q_i} . \square

5. MUTATION AND THE ALMOST TORIC GEOMETRY OF \mathbb{CP}^2

In this section, we will give two additional, self-contained, proofs that X_{p_1, p_2, p_3} is diffeomorphic to \mathbb{CP}^2 , and hence two more proofs of Theorem 1.1. The first proof is based on almost toric geometry, though does not actually use it. We begin in Section 5.1 by giving this alternate proof.

In Section 5.2, we give an overview of almost toric pictures and discuss Vianna's [26, 27] construction of infinitely many almost toric pictures of \mathbb{CP}^2 corresponding to Markov triples. We will give explicit handle descriptions corresponding to these almost toric pictures of \mathbb{CP}^2 and transferring the cut (giving yet another proof that X_{p_1, p_2, p_3} is diffeomorphic to \mathbb{CP}^2) in Section 5.3. In the literature the relationship between almost toric pictures and symplectic handlebodies has been studied for Weinstein domains [1], but not for closed symplectic manifolds. This handlebody description of transferring the cut is what lies behind our proof of Theorem 1.1 in Section 5.1.

Finally in Section 5.4, we will see that the symplectic structure coming from our symplectic handlebody decomposition can be deformed so that one can explicitly see the Lagrangian almost toric fibration, which completes the proof of Theorem 1.2.

5.1. Mutation moves in handlebody pictures. Motivated by moves in almost toric geometry, we will show that if two Markov triples (p_1, p_2, p_3) and (p'_1, p'_2, p'_3) are related by a mutation (see Section 2.1), then X_{p_1, p_2, p_3} and $X_{p'_1, p'_2, p'_3}$ are diffeomorphic. This in turn shows that all the X_{p_1, p_2, p_3} are diffeomorphic to \mathbb{CP}^2 , thus giving another proof of Theorem 4.6 independent of the work of Lisca and Parma [21].

Proposition 5.1. *The manifolds X_{p_1, p_2, p_3} and X_{p_2, p_3, p'_1} , constructed in Section 3.3, corresponding to two mutation-related Markov triples (p_1, p_2, p_3) and (p_2, p_3, p'_1) , where $p'_1 = 3p_2p_3 - p_1$, are diffeomorphic. Also, X_{p_1, p_2, p_3} and X_{p_1, p_3, p'_2} , corresponding to two mutation-related Markov triples (p_1, p_2, p_3) and (p_1, p_3, p'_2) , where $p'_2 = 3p_1p_3 - p_2$, are diffeomorphic.*

We will first show that Proposition 5.1 implies Theorem 4.6, independent of Section 4.

Proof of Theorem 4.6. Consider $X_{1,1,1}$. We first show that it is diffeomorphic to \mathbb{CP}^2 . We are using $x = 1$ and $y = 0$ in the proof of Proposition 3.8 and obtain $q_1 = 0$ and $q_2 = q_3 = 3$. Following the construction from Section 3.1, we attach a 2-handle along $(1, -1)$ -torus knot in $L(1, 2) = \partial B_{1,3} \cong \partial B^4 = S^3$ with the torus framing. We can see that it is an unknot in S^3 with framing $+1$ with respect to the Seifert framing. After that, we attach the upside down handlebody $B_{1,1} \natural B_{1,2} \cong B^4$ and clearly the resulting manifold is \mathbb{CP}^2 .

Notice that for the two mutations, (p_2, p_3, p'_1) is a left child of (p_1, p_2, p_3) and (p_1, p_3, p'_2) is a right child of (p_1, p_2, p_3) in the Markov tree as shown in Figure 2. Thus for any X_{p_1, p_2, p_3} , we have a sequence of mutations that relates the Markov triples (p_1, p_2, p_3) and $(1, 1, 1)$. By repeated application of Proposition 5.1, we see that X_{p_1, p_2, p_3} is diffeomorphic to \mathbb{CP}^2 . Then, as in the proof of Theorem 1.1, by the result of Taubes [25, Theorem 0.3], it follows that X_{p_1, p_2, p_3} is symplectomorphic to \mathbb{CP}^2 after scaling the symplectic form. \square

Proposition 5.1 will follow from the next lemma. Recall the pants cobordism W_{p_1, q_1, p_2, q_2} defined in Section 4.2. We define Z_{p_1, q_1, p_2, q_2} to be the union of W_{p_1, q_1, p_2, q_2} , B_{p_1, q_1} and B_{p_2, q_2} as described in Figure 12.

Lemma 5.2. *Let $p_1, p_2, p'_1, p'_2, p_3$ be as in the statement of Proposition 5.1 and q_1, q_2 be defined as in Proposition 3.8 for (p_1, p_2, p_3) . Let q'_1 be the appropriate number for the embedding corresponding to the (p_2, p_3, p'_1) triple, coming from Proposition 3.8. Define q'_2 similarly. Then, the three smooth manifolds Z_{p_1, p_2, q_1, q_2} , $Z_{p'_2, p_1, q'_2, q_1}$ and $Z_{p'_1, p_2, q'_1, -q_2}$ are diffeomorphic.*

Proof. We first show that Z_{p_1, p_2, q_1, q_2} and $Z_{p'_1, p_2, q'_1, -q_2}$ are diffeomorphic. Denote a (p, q) torus knot in $\partial(S^1 \times D^3)$ by $K_{p, q}$. Consider the coordinates on $S^1 \times D^3$ to be (θ, x, y, z) . Then $\partial(S^1 \times D^3) = \{(\theta, x, y, z) \mid x^2 + y^2 + z^2 = 1\}$. The pictures represent that $K_{p_2, -q_2}$ lives on a Heegaard torus

$$T_2 := \{(\theta, x_2, y, z) \mid y^2 + z^2 = 1 - x_2^2\}$$

and K_{p_1, q_1} lives on a Heegaard torus

$$T_1 := \{(\theta, x_1, y, z) \mid y^2 + z^2 = 1 - x_1^2\}$$

such that $x_2 < x_1$. Consider the self-diffeomorphism $\phi : S^1 \times D^3 \rightarrow S^1 \times D^3$ given by $\phi(\theta, x, y, z) = (\theta, -x, y, -z)$. Then, $\phi(K_{p_2, -q_2}) = K_{p_2, q_2}$. Similarly, $\phi(K_{p_1, q_1}) = K_{p_1, -q_1}$. However the order of the x -coordinates of the Heegaard tori they live on have been flipped. To get the knots in the same order as the manifold in Figure 13, $\phi(K_{p_1, q_1}) = K_{p_1, -q_1}$ needs to be slid past the surgery on $\phi(K_{p_2, -q_2}) = K_{p_2, q_2}$.

Recall, Lemma 2.14 says, a (-1) -surgery on a knot on the Heegaard torus is the same as cutting and regluing by a $(+1)$ -Dehn twist along the knot. So pushing $\phi(K_{p_1, q_1}) = K_{p_1, -q_1}$ past the Heegaard torus on which $\phi(K_{p_2, -q_2}) = K_{p_2, q_2}$ sits will result in the following torus knot (p'_1, q'_1) as the following computation, which heavily uses Proposition 3.8, shows:

$$\begin{aligned} \begin{pmatrix} 1 + p_2 q_2 & -q_2^2 \\ p_2^2 & 1 - p_2 q_2 \end{pmatrix} \begin{pmatrix} -q_1 \\ p_1 \end{pmatrix} &= \begin{pmatrix} -p_1 q_2^2 - q_1 - p_2 q_2 q_1 \\ p_1 - p_2 q_2 p_1 - p_2^2 q_1 \end{pmatrix} \\ &= - \begin{pmatrix} 3q_2 p_3 + q_1 \\ 3p_2 p_3 - p_1 \end{pmatrix} \\ &= - \begin{pmatrix} q'_1 \\ p'_1 \end{pmatrix} \end{aligned}$$

The only computation above that does not directly follow from the definition of mutation and Proposition 3.8 is that $3q_2 p_3 + q_1 = q'_1$. Recall that the p_i 's and q_i 's satisfy the conditions in Proposition 3.8. Note that $q'_1 = 2p_3 y'$ where $y' = 3p_3 x + y$ since $p'_1(-x) + p_2 y' = p'_1(-x) + p_2(3p_3 x + y) = (3p_2 p_3 - p_1)(-x) + 3p_2 p_3 x + p_2 y = 1$ and so

$$\begin{aligned} q'_1 &= 3p_3 y' \\ &= 3p_3(3p_3 x + y) \\ &= 3q_2 p_3 + q_1 \end{aligned}$$

Thus verifying that the conditions in Proposition 3.8 are satisfied, it follows that the manifold obtained after the diffeomorphism is exactly $Z_{p'_1, p_2, q'_1, -q_2}$.

To prove the diffeomorphism between Z_{p_1, p_2, q_1, q_2} and $Z_{p'_2, p_1, q'_2, q_1}$, we need to slide the knot $K_{p_2, -q_2}$ in Z_{p_1, p_2, q_1, q_2} past the surgery on K_{p_1, q_1} . This results in exactly the (p'_2, q'_2) torus knot, by doing the same matrix arguments as above but interchanging p_1 and p_2 , and q_1 and q_2 . The resultant manifold is then $Z_{p'_2, p_1, q'_2, q_1}$. \square

Proof of Proposition 5.1. Notice that Z_{p_1, p_2, q_1, q_2} , $Z_{p'_2, p_1, q'_2, q_1}$, and $Z_{p'_1, p_2, q'_1, -q_2}$, all have boundary $L(p_3^2, -p_3 q_3 + 1)$. Thus gluing in the homology ball B_{p_3, q_3} bounded by $L(p_3^2, p_3 q_3 - 1)$ extends the diffeomorphisms and identifies $X_{p_1, p_2, p_3}, X_{p_1, p_3, p'_2}, X_{p_2, p_3, p'_1}$. \square

5.2. Almost toric pictures of \mathbb{CP}^2 . Symington [24] introduced *almost toric manifolds* as a way to "see" certain symplectic manifolds as their images under a moment map; this generalized the pre-existing notion of toric manifolds. The idea is to define a Lagrangian fibration structure on a symplectic manifold (M, ω) where a regular fiber is a Lagrangian torus, some of the fibers are pinched tori referred to as *nodal singularities*. More precisely:

Definition 5.3. (Vianna [26, Definition 2.9]) An *almost toric fibration* of a symplectic four manifold (M, ω) is a Lagrangian fibration $\pi : (M, \omega) \rightarrow B$ such that any point of (M, ω) has a Darboux neighborhood (with symplectic form $dx_1 \wedge dy_1 + dx_2 \wedge dy_2$) in which the map π has one of the following forms:

$\pi(x, y) = (x_1, x_2),$	regular point
$\pi(x, y) = (x_1, x_1^2 + x_2^2),$	elliptic, corank one
$\pi(x, y) = (x_1^2 + x_2^2, x_2^2 + y_2^2),$	elliptic, corank two
$\pi(x, y) = (x_1 y_1 + x_2 y_2, x_1 y_2 - x_2 y_1),$	nodal or focus-focus

with respect to some choice of coordinates near the image point in B . An *almost toric manifold* is a symplectic manifold equipped with an almost toric fibration. A *toric fibration* is a Lagrangian fibration induced by an effective Hamiltonian torus action.

We call the image of each nodal singularity a *node*. We will now discuss how to reconstruct the symplectic manifold from the base B . Figure 14 is an example of B for an almost toric fibration, ignore the blue curves for now.

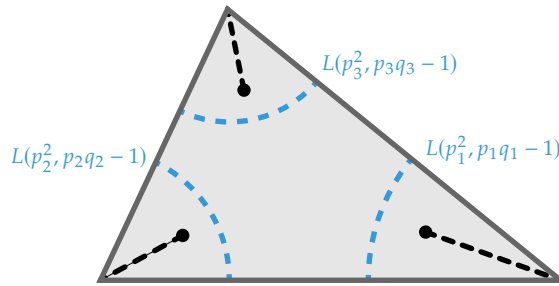


FIGURE 14. An almost toric picture of \mathbb{CP}^2 corresponding to the Markov triple (p_1, p_2, p_3) .

The pre-image of a regular point in the interior of the triangle is a Lagrangian torus, while the pre-image of a point in the interior of an edge is an isotropic circle (these are elliptic, corank one points). As one approaches a point on the interior of an edge from the interior of the polytope all circles of a fixed slope in the torus collapses to leave the circle above the edge. The circle that collapses is given by the integral normal vector to the line. The pre-image of a vertex is a point (these are elliptic, corank two points) and the pre-image of a node is a pinched torus. The dotted lines from the nodes to the vertices encode the slope of the curve on a regular torus fiber that collapses in the singular fiber corresponding to that node. This dotted line is called an *eigenline*. Its eigendirection $\pm(a, b)$ encodes the monodromy $A_{(a,b)} = \begin{pmatrix} 1 - ab & a^2 \\ -b^2 & 1 + ab \end{pmatrix}$ in the affine structure of the base when going around the node – the eigenline, as the name suggests, is invariant

under the monodromy, while the slopes of the boundary on either side of the point where the eigenline hits the boundary, should be related by counterclockwise rotation given by the monodromy. This means that the slope on the right, after being rotated by $A_{(a,b)}$, should match the slope on the left. More specifically, consider the toric diagram and cut the manifold along the pre-image of the dotted line and then reglue the fibers by the affine transformation $A_{(a,b)}$. This will make a small neighborhood of a corner with a dotted line into an $S^1 \times D^3$ and when that neighborhood is expanded to contain the node, one attaches a 2-handle with framing -1 less than the torus framing to the (a, b) sloped curve sitting on a torus in $S^1 \times S^2$. Thus we see a neighborhood of a dotted line is a rational homology ball with boundary a lens space.

Toric Moves. We discuss three moves that can be done to an almost toric diagram without changing the manifold. With these three moves we can reproduce Vianna's embeddings of rational homology balls associated to a Markov triple into \mathbb{CP}^2 .

Nodal trade. In Figure 15 we see the standard toric diagram for a Darboux ball B^4 and an almost toric picture that can easily be seen to be B^4 as well and can also be shown to be a Darboux ball as well. A *nodal trade* is the operation of exchanging one picture for the other. See [24, Section 6] for more details.

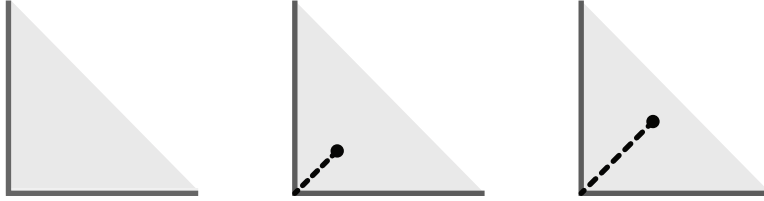


FIGURE 15. On the left is the standard toric picture for a Darboux ball. In the middle is an almost toric picture for the Darboux ball. A nodal trade exchanges one of these pictures for the other. Going between the middle and the right hand picture is a nodal slide.

Nodal slide. A *nodal slide* simply lengthens or shortens an eigenline. See [24, Section 6] for more details.

Transfer the cut. The description here follows [24, 27], and the reader should refer there for more details. Recall a node in the base diagram of an almost toric diagram has an associated eigenline in some eigendirection (a, b) , this is the dotted line in the diagram. Notice that there are two line segments leaving the node x in the direction (a, b) , the original eigenline E and a line segment L on the opposite side of x .

One can cut B along $E \cup L$, and apply an affine transformation to one of the pieces so that the vertex that E touched becomes the interior point of an edge and L will now be an eigenline connecting the node x to a corner in the new base diagram. See Figure 16.

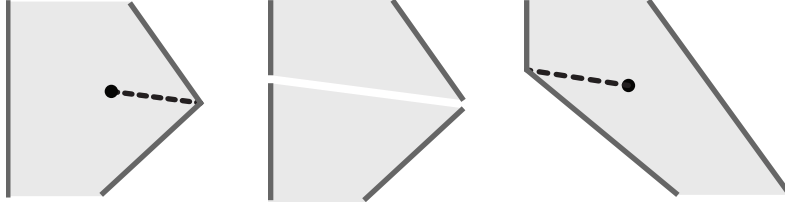


FIGURE 16. Transfer the cut. On the left we see a portion of an almost toric diagram. In the middle we have cut the diagram along the eigendirection for the node. On the right we have reglued the two pieces so that the eigenline now leave the opposite side of the node.

We can now start with the standard toric picture for \mathbb{CP}^2 , see the upper left in Figure 17. We can now perform nodal trades at each corner point to obtain an almost toric diagram for \mathbb{CP}^2 .

Near each corner, one can see S^3 as the preimage of the boundary of a neighborhood of the corner, thus this is the almost toric picture corresponding to the Markov triple $(1, 1, 1)$. One can then perform an operation called transferring the cut (and nodal slide).

We show this in Figure 17, this changes the almost toric picture to one where one of the corners now represents $B_{2,1}$, with boundary $L(4, 1)$ — this corresponds to the Markov triple $(1, 1, 2)$. In general, this procedure allows one to build an almost toric picture of \mathbb{CP}^2 corresponding to any Markov triple (p_1, p_2, p_3) — this follows from the fact that all Markov triples can be obtained via mutations from $(1, 1, 1)$. Further, as shown in Figure 14, this picture also encodes the embedding of $\sqcup_{i=1}^3 B_{p_i, q_i}$ into \mathbb{CP}^2 . In the next subsection we will see how to draw handlebody decompositions associated to almost toric pictures and give a handlebody interpretation of transferring the cut and see that the proof of Proposition 5.1 is simply transferring the cut.

5.3. From almost toric pictures to handlebody decompositions. We will first understand a handle decomposition of the complement of a rational homology ball associated to a nodal singularity.

Proposition 5.4. *Consider \mathbb{CP}^2 with the almost toric structure corresponding to the Markov triple (p_1, p_2, p_3) shown in Figure 14. The complement of the rational homology ball B_{p_3, q_3} has a handle decomposition given in Figure 10 and hence also Figure 12.*

Proof. As discussed in the previous section, the rational homology ball associated to each nodal singularity has a handle decomposition with one handle in each index 0, 1, and 2. Moreover the 2-handle is attached to a (p_i, q_i) torus knot in $S^1 \times S^2$. So these are precisely the B_{p_i, q_i} from Section 2.6. Thus we understand handle decompositions of the parts of \mathbb{CP}^2 above the regions separated off of the almost toric diagram by the dotted blue curves in Figure 18. If one adds the region H above the dark grey portion in Figure 18 to

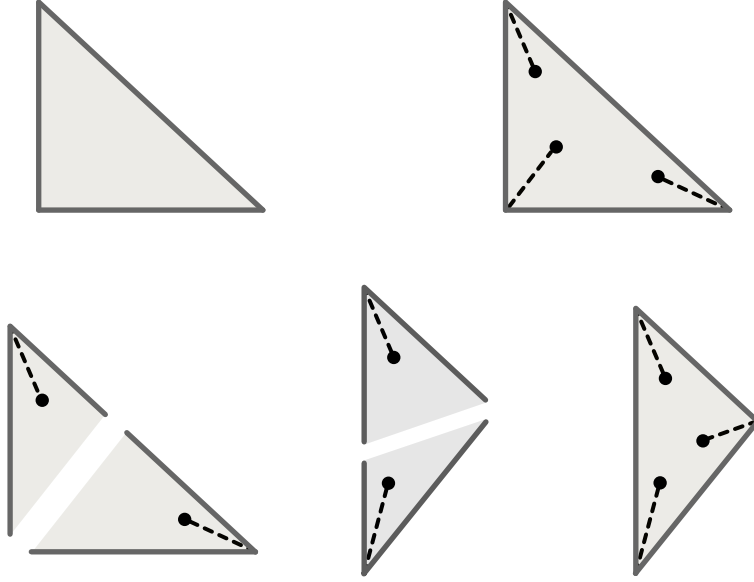


FIGURE 17. In the upper left is the standard toric picture of \mathbb{CP}^2 . In the upper right we have performed nodal trades to get an almost toric diagram for \mathbb{CP}^2 for the Markov triple $(1, 1, 1)$ (a neighborhood of each dotted line is B^4). In the bottom left we cut along the diagram along eigenline for the bottom left node. In the middle figure we applied the monodromy to the bottom piece of the diagram. On the bottom right we see the result of the transferring the cut and nodal slide, which gives the mutated Markov triple $(1,1,2)$.

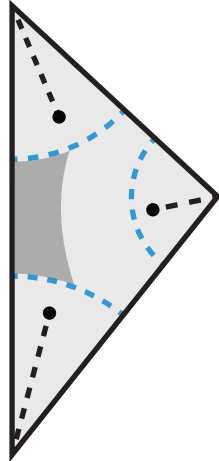


FIGURE 18. The round 1-handle seen in the almost toric picture.

the two rational homology balls that it touches, then the result will be diffeomorphic to the complement of the third rational homology ball.

Notice that H is $S^1 \times D^3$ and it is attached to the two rational homology balls along $S^0 \times S^1 \times D^2$, that is along an $S^1 \times D^2$ in each rational homology ball. This is called a *round 1-handle*. It is easy to see the circles the round 1-handle are attached to are rational unknots in the two lens spaces (that is cores of Heegaard tori for the lens spaces) and that the framing on each is the zero framing (the toric structure frames the rational unknots and the attaching regions of the handle). Now a round 1-handle can be decomposed into a standard 1-handle and a standard 2-handle. The 1-handle is attached to points on each of the rational unknots and cancels one of the 0-handles of one of the rational homology balls. This gives Figure 10 without the yellow curve. Notice that after the 1-handle is attached the 2-handle will be attached to the connect sum of the rational unknots, and this is exactly the yellow curve in the figure. Moreover, the zero framings of the attaching regions gives use the fact that the yellow 2-handle should have framing 0. That is Figure 10 indeed does describe the complement of one of the rational homology balls as claimed. \square

We now have a third proof of Theorem 4.6, and Theorem 1.2, that the manifold X_{p_1, p_2, p_3} we constructed in Section 3.3 are diffeomorphic to \mathbb{CP}^2 .

Corollary 5.5. *The manifolds X_{p_1, p_2, p_3} constructed in Section 3.3 are diffeomorphic to \mathbb{CP}^2 .*

Proof. Given a Markov triple (p_1, p_2, p_3) the rational homology balls in X_{p_1, p_2, p_3} and in \mathbb{CP}^2 with the almost toric structure associated to the triple are the same. Moreover, the previous proposition shows us that the complement of B_{p_3, q_3} in each are both obtained by attaching the same round 1-handle to $B_{p_1, q_1} \cup B_{p_2, q_2}$ and thus they are diffeomorphic. Since any diffeomorphism of $\partial B_{p_3, q_3}$ extends over B_{p_3, q_3} , see Item (2) in Remark 2.15, we know that X_{p_1, p_2, p_3} is diffeomorphic to \mathbb{CP}^2 . \square

Transferring the cut in handlebody diagrams of \mathbb{CP}^2 . Notice that when transferring the cut, only two of the nodal singularities are involved, and hence only two of the rational homology balls. Specifically, there is the node that is being transferred and there is the node that has an affine transformation applied to it (the third node is unaffected). So we only need to consider the complement of one of the rational homology balls when studying transfer the cut. We know from Proposition 5.4 that this complement is $S^1 \times D^3$ with two 2-handles attached, where the attaching circles of the 2-handles correspond to the eigenlines of the nodes. Given an almost toric picture for \mathbb{CP}^2 the attaching curves of the 2-handles occur on separate Heegaard tori in $S^1 \times S^2$ and the order of those tori is important and is determined by the order on the nodal singularities. Transferring the cut corresponds to changing this order, but when one does this, one must apply the associated monodromy $A_{(p_i, q_i)}$ to the other attaching circle, this corresponds to the handle slide in the proof of Lemma 5.2. Similarly, one can read the curves in the opposite order (this

corresponds to the diffeomorphism ϕ in the proof of Lemma 5.2). This is the almost toric geometry inspiration for the proof of Lemma 5.2.

5.4. From handle descriptions to almost toric pictures. Recall from Section 3.3 that X_{p_1, p_2, p_3} admits a symplectic handlebody decomposition for each Markov triple (p_1, p_2, p_3) . The following proposition shows that X_{p_1, p_2, p_3} admits a smooth fibration by tori (and three singular tori) and after a deformation of the symplectic structure, we can arrange that this is a Lagrangian (almost toric) fibration.

Proposition 5.6. *For each Markov triple (p_1, p_2, p_3) , after a deformation of the symplectic structure ω_{p_1, p_2, p_3} there is a smooth map from X_{p_1, p_2, p_3} to \mathbb{R}^2 , with the generic pre-image of a point being a Lagrangian torus, and the identification of X_{p_1, p_2, p_3} with \mathbb{CP}^2 in Corollary 5.5. This fibration agrees with the almost toric fibration of \mathbb{CP}^2 corresponding to the Markov triple (p_1, p_2, p_3) .*

Proof. We know that each B_{p_i, q_i} admits an almost toric fibration by Lagrangian tori from our discussion in Section 5.2. Moreover we know the round 1-handle discussed in the proof of Proposition 5.4 admits a toric fibration. The round 1-handle used in our construction of X_{p_1, p_2, p_3} possibly has a different symplectic structure on it, but it will nonetheless have a smooth toric fibration that extends the toric fibrations on the B_{p_i, q_i} . Thus the diffeomorphism from X_{p_1, p_2, p_3} to \mathbb{CP}^2 in Corollary 5.5 takes torus fibers to torus fibers. The pull-back of the symplectic form on \mathbb{CP}^2 will be deformation equivalent to the one we constructed ω_{p_1, p_2, p_3} by Taubes theorem [25, Theorem 0.3] and this completes the proof. \square

This establishes that the two descriptions of \mathbb{CP}^2 , coming from X_{p_1, p_2, p_3} and the almost toric picture corresponding to the Markov triple, are analogous.

Proof of Theorem 1.2. The statement of Theorem 1.2 follows from Proposition 5.6. \square

REFERENCES

- [1] Bahar Acu, Orsola Capovilla-Searle, Agnès Gadbled, Aleksandra Marinković, Emmy Murphy, Laura Starkston, and Angela Wu. Weinstein handlebodies for complements of smoothed toric divisors, 2022. [arXiv:2012.08666](#).
- [2] Martin Aigner. *Markov's theorem and 100 years of the uniqueness conjecture*. Springer, Cham, 2013. A mathematical journey from irrational numbers to perfect matchings.
- [3] Kenneth L. Baker, John B. Etnyre, and Jeremy Van Horn-Morris. Cabling, contact structures and mapping class monoids. *J. Differential Geom.*, 90(1):1–80, 2012.
- [4] John A. Baldwin and John B. Etnyre. Admissible transverse surgery does not preserve tightness. *Math. Ann.*, 357(2):441–468, 2013.
- [5] Apratim Chakraborty, John B. Etnyre, and Hyunki Min. Cabling legendrian and transverse knots, 2020. [arXiv:2012.12148](#).
- [6] James Conway. Transverse surgery on knots in contact 3-manifolds. *Trans. Amer. Math. Soc.*, 372(3):1671–1707, 2019.
- [7] Yakov Eliashberg. Topological characterization of Stein manifolds of dimension > 2 . *Internat. J. Math.*, 1(1):29–46, 1990.

- [8] John B. Etnyre and Ko Honda. Knots and contact geometry. I. Torus knots and the figure eight knot. *J. Symplectic Geom.*, 1(1):63–120, 2001.
- [9] John B. Etnyre and Ko Honda. On symplectic cobordisms. *Math. Ann.*, 323(1):31–39, 2002.
- [10] John B. Etnyre, Hyunki Min, and Anubhav Mukherjee. Non-loose torus knots, 2022. [arXiv:2206.14848](#).
- [11] John B. Etnyre and David Shea Vela-Vick. Torsion and open book decompositions. *Int. Math. Res. Not. IMRN*, 2010(22):4385–4398, 2010.
- [12] Jonathan Evans and Ivan Smith. Markov numbers and lagrangian cell complexes in the complex projective plane. *Geometry & Topology*, 22(2):1143–1180, 2018.
- [13] David T. Gay. Symplectic 2-handles and transverse links. *Trans. Amer. Math. Soc.*, 354(3):1027–1047, 2002.
- [14] Hansjörg Geiges and Sinem Onaran. Legendrian rational unknots in lens spaces. *J. Symplectic Geom.*, 13(1):17–50, 2015.
- [15] Emmanuel Giroux. Structures de contact en dimension trois et bifurcations des feuilletages de surfaces. *Invent. Math.*, 141(3):615–689, 2000.
- [16] Robert E. Gompf. Handlebody construction of Stein surfaces. *Ann. of Math. (2)*, 148(2):619–693, 1998.
- [17] Ko Honda. On the classification of tight contact structures. I. *Geom. Topol.*, 4:309–368, 2000.
- [18] Yutaka Kanda. The classification of tight contact structures on the 3-torus. *Comm. Anal. Geom.*, 5(3):413–438, 1997.
- [19] YankıLekili and Maksim Maydanskiy. The symplectic topology of some rational homology balls. *Comment. Math. Helv.*, 89(3):571–596, 2014.
- [20] Paolo Lisca and Andrea Parma. Horizontal decompositions, I, 2022. [arXiv:2205.00482](#).
- [21] Paolo Lisca and Andrea Parma. Horizontal decompositions, II, 2023. [arXiv:2302.14606](#).
- [22] Hyunki Min. The contact mapping class group and rational unknots in lens spaces, 2022. [arXiv:2207.03590](#).
- [23] Dale Rolfsen. *Knots and links*. Mathematics Lecture Series, No. 7. Publish or Perish, Inc., Berkeley, Calif., 1976.
- [24] Margaret Symington. Four dimensions from two in symplectic topology. In *Topology and geometry of manifolds (Athens, GA, 2001)*, volume 71 of *Proc. Sympos. Pure Math.*, pages 153–208. Amer. Math. Soc., Providence, RI, 2003.
- [25] Clifford H. Taubes. $SW \Rightarrow Gr$: from the Seiberg-Witten equations to pseudo-holomorphic curves. *J. Amer. Math. Soc.*, 9(3):845–918, 1996.
- [26] Renato Vianna. On exotic Lagrangian tori in \mathbb{CP}^2 . *Geom. Topol.*, 18(4):2419–2476, 2014.
- [27] Renato Vianna. Infinitely many monotone Lagrangian tori in del Pezzo surfaces. *Selecta Math. (N.S.)*, 23(3):1955–1996, 2017.
- [28] Jonathan Wahl. Smoothings of normal surface singularities. *Topology*, 20(3):219–246, 1981.
- [29] Alan Weinstein. Contact surgery and symplectic handlebodies. *Hokkaido Math. J.*, 20(2):241–251, 1991.

SCHOOL OF MATHEMATICS, GEORGIA INSTITUTE OF TECHNOLOGY, ATLANTA, GA

Email address: etnyre@math.gatech.edu

Email address: aroy86@gatech.edu

DEPARTMENT OF MATHEMATICS, UNIVERSITY OF CALIFORNIA, LOS ANGELES, CA

Email address: hkmin27@math.ucla.edu

DEPARTMENT OF MATHEMATICS, MASSACHUSETTS INSTITUTE OF TECHNOLOGY, CAMBRIDGE, MA

Email address: piccirli@mit.edu